Protective effects of milk thistle (Sylibum marianum) seed oil and α-tocopherol against 7β-hydroxycholesterol-induced peroxisomal alterations in murine C2C12 myoblasts: Nutritional insights associated with the concept of pexotherapy

Imen Ghzaiel, Amira Zarrouk, Soukaina Essadek, Lucy Martine, Souha Hammouda, Aline Yammine, Mohamed Ksila, Thomas Nury, Wiem Meddeb, Mounia Tahri Joutey, et al.

Protective effects of milk thistle (*Sylibum marianum*) seed oil and α-tocopherol against 7β-hydroxycholesterol-induced peroxisomal alterations in murine C2C12 myoblasts: nutritional insights associated with the concept of pexotherapy

Imen Ghzaiel [a,b,c], Amira Zarrouk [b,d **], Soukaina Essadek [a,e], Lucy Martine [f], Souha Hammouda [b], Aline Yammine [a, g], Mohamed Ksila [a,c], Thomas Nury [a], Wiem Meddeb [a], Mounia Tahri Joutey[a,e], Wafa Mihoubi [h], Claudio Caccia [i], Valerio Leoni [i], Mohammad Samadi [j], Niyazi Acar [f], Pierre Andreoletti [a], Sonia Hammami [b], Taoufik Ghrairi [c], Anne Vejux [a], Mohamed Hammami [b], Gérard Lizard [a*]

[a] Team 'Biochemistry of the Peroxisome, Inflammation and Lipid Metabolism' EA7270/Inserm, University Bourgogne Franche-Comté, 21000 Dijon, France

[b] Lab-NAFS 'Nutrition—Functional Food & Vascular Health', Faculty of Medicine, University of Monastir, LR12ES05, 5000 Monastir, Tunisia

[c] Faculty of Sciences of Tunis, University Tunis-El Manar, 2092 Tunis, Tunisia

[d] Faculty of Medicine, University of Sousse, 4000 Sousse, Tunisia

[e] Laboratory of Biochemistry, Neurosciences, Natural Resources and Environment, Faculty of Sciences & Techniques, University Hassan I, BP 577, 26000 Settat, Morocco

[f] Centre des Sciences du Goût et de l'Alimentation, AgroSup Dijon, CNRS, INRAE, Université Bourgogne Franche-Comté, 21065 Dijon, France

[g] Bioactive Molecules Research Laboratory, Doctoral School of Sciences and Technologies, Faculty of Sciences, Lebanese University, Fanar, Jdeidet P.O. Box 90656, Lebanon

[h] Laboratoire de Biotechnologie Moléculaire des Eucaryotes; Centre de Biotechnologie de Sfax; B.P 1177; Université de Sfax, 3018 Sfax, Tunisia

[i] Laboratory of Clinical Chemistry, Hospitals of Desio, ASST-Brianza and Department of Medicine and Surgery, University of Milano-Bicocca, 20900 Monza

[j] LCPMC-A2, ICPM, Department of Chemistry, University Lorraine, Metz Technopôle, 57070 Metz, France

* ***Corresponding author and co-corresponding author associated at***: * Dr Gérard LIZARD, E-mail: gerard.lizard@u-bourgogne.fr Tel.: +33-380-396-256; ** Dr Amira ZARROUK, E-mail: zarroukamira@gmail.com

ABSTRACT

Peroxisomes play an important role in regulating cell metabolism and RedOx homeostasis. Peroxisomal dysfunctions favor oxidative stress and cell death. The ability of 7β-hydroxycholesterol (7β-OHC; 50 µM, 24 h), known to be increased in patients with age-related diseases such as sarcopenia, to trigger oxidative stress, mitochondrial and peroxisomal dysfunction was studied in murine C2C12 myoblasts. The capacity of milk thistle seed oil (MTSO, 100 µg/mL) as well as α-tocopherol (400 µM; reference cytoprotective agent) to counteract the toxic effects of 7β-OHC, mainly at the peroxisomal level were evaluated. The impacts of 7β-OHC, in the presence or absence of MTSO or α-tocopherol, were studied with complementary methods: measurement of cell density and viability, quantification of reactive oxygen species (ROS) production and transmembrane mitochondrial potential (ΔΨm), evaluation of peroxisomal mass as well as topographic, morphologic and functional peroxisomal changes. Our results indicate that 7β-OHC induces a loss of cell viability and a decrease of cell adhesion associated with ROS overproduction, alterations of mitochondrial ultrastructure, a drop of ΔΨm, and several peroxisomal modifications. In the presence of 7β-OHC, comparatively to untreated cells, important quantitative and qualitative peroxisomal modifications were also identified: a) a reduced number of peroxisomes with abnormal sizes and shapes, mainly localized in cytoplasmic vacuoles, were observed; b) the peroxisomal mass was decreased as indicated by lower protein and mRNA levels of the peroxisomal ABCD3 transporter; c) lower mRNA level of *Pex5* involved in peroxisomal biogenesis as well as higher mRNA levels of *Pex13* and *Pex14,* involved in peroxisomal biogenesis and/or pexophagy, was found; d) lower levels of ACOX1 and MFP2 enzymes, implicated in peroxisomal β-oxidation, were detected; e) higher levels of very-long-chain fatty acids, which are substrates of peroxisomal β-oxidation, were found. These different cytotoxic effects were strongly attenuated by MTSO, in the same range of order as with α-tocopherol. These findings underline the interest of MTSO and α-tocopherol in the prevention of peroxisomal damages (pexotherapy).

Key words: 7β-hydroxycholesterol, C2C12 myoblasts, milk thistle seed oil, peroxisome, pexotherapy, sarcopenia.

1-Introduction

Due to the increase in life expectancy, which is multifactorial with important differences between men and women whatever the country considered [1] [2], the incidence of age-related diseases is increasing [3] [4]. These include cardiovascular diseases associated with atherosclerosis, type 2 diabetes which is also influenced by nutritional habits, certain neurodegenerative diseases (Alzheimer's disease, Parkinson's disease), eye diseases (age-related macular degeneration (AMD), cataract), osteoporosis, sarcopenia, and certain cancers such as prostate cancer [5] [6]. In addition, ageing depends both on genetic and extrinsic risk factors which can contribute to obesity and favor COVID-19 infections mainly in the elderly, leading to serious complications and sometimes fatal outcomes [7]. Some of these diseases (cardiovascular, neurodegenerative, AMD, cataract, sarcopenia) are associated with an enhancement of the oxidative stress not only at the lesion and/or tissue level, but also systemically [5]. This oxidative stress, which leads to an overproduction of reactive oxygen species (ROS) and sometimes reactive nitrogen species (RNS), favors lipid peroxidation and can induce the carbonylation of proteins and the formation of 8-hydroxyguanine at the DNA level, which predisposes to mutations [8] [9] [10]. The auto-oxidation of cholesterol can also lead to the formation of oxidized derivatives, called oxysterols [11], which can be considered as important but underestimated components of the exposome whose composition can influence ageing [12]. Due to the double bond in the 5,6 position on the sterane ring of cholesterol, free radical attack on carbon 7 is most likely and leads to the formation of 7-ketocholesterol (7KC) but also 7β-hydroxycholesterol (7β-OHC), these two oxysterols being interconvertible via the enzymes 7β-hydroxycholesterol dehydrogenase-1 (7β-HSD1: conversion of 7KC to 7β-OHC) and 7β-hydroxycholesterol dehydrogenase-2 (7β-HSD2:

conversion of 7β-OHC to 7KC) [13] [14]. In cardiovascular diseases, Alzheimer's disease, AMD and cataract, severe forms of SARS-CoV2 and sarcopenia, increased levels of 7KC and 7β-OHC have been found at the lesion site and/or plasma level [15] [16] [17] [18]. In addition, it has been shown that 7KC levels can permit distinction between normal and pathological ageing [19] [20]. Currently, in some age-related diseases (cardiovascular diseases, Alzheimer's disease, and AMD), the involvement of 7KC and/or 7β-OHC in the pathophysiology is widely suspected since these oxysterols can initiate signal transduction pathways that are relevant to the development of these diseases [21] [14]. In sarcopenia, plasma increases in 7β-OHC and 7KC have also been observed, with the increase in 7β-OHC being significant [22]. In sarcopenia, which contributes to the loss of autonomy in the elderly and is associated with a loss of mobility representing a serious handicap [23], a better understanding of the effects of 7β-OHC on myogenesis is an important issue. In this context, the effects of 7β-OHC on skeletal muscle need to be clarified.

For this purpose, murine C2C12 myoblasts were chosen as a model. In these cells, we have previously shown that 7β-OHC induces cell death associated with strong oxidative stress (overproduction of ROS) leading to mitochondrial and peroxisomal dysfunctions [22]. These different cellular alterations induced by 7β-OHC are strongly attenuated by the *Pistacia Lentiscus* L. seed oil (PLSO) often used in Tunisian cooking but also by α-tocopherol known for its cytoprotective effects on different types of cells treated with toxic oxysterols (7KC, 7β-OHC and 24S-hydroxycholesterol (24S-OHC)) [24] [25] [26]. Among the oils from the Mediterranean basin, milk thistle seed oil (MTSO) has been used for a long time in traditional medicine, in particular, to treat liver disorders [27]. The hepatoprotective effect of MTSO could be mainly due to sylibin. This molecule which is a flavonolignan, is the main component but also the most active ingredient of milk thistle (Sylibum marianum) fruit extract (silymarin) [28]. MTSO,

regardless of where the seeds are collected in Tunisia, is richer in α-tocopherol than Tunisian olive oil and its concentration can be higher than in argan oils from Morocco [29] [30]. Based on several tests of anti-oxidant activities (DPPH (2,2-diphenyl-1-picrylhydrazyl), FRAP (ferric reducing-antioxidant power), KRL (Kit radicaux libres), and CPFI (chelation power on ferrous ions)), MTSO also showed a very good anti-oxidant profile [30] [31]. In the context of the prevention of neurodegeneration, we also have already demonstrated on 158N murine oligodendrocytes treated with 7KC that MTSO prevents cell death by oxiapoptophagy involving OXIdative stress, APOPTOsis and autoPHAGY [32] [33] [34] [35]. However, the biological activities of MTSO are still poorly studied on other cells, such as skeletal muscle cells, in the context of the prevention of age-related diseases by considering in particular its impact on organelles.

To this end, in the present study, the cytoprotective effects of MTSO (obtained by Meddeb W. *et al.* [29] from seeds collected in the area of Sousse and characterized by Zarrouk A. *et al.* [30]) as well as of α-tocopherol (present at a high concentration in MTSO (441.23 ± 46.59 µM) and used as a reference cytoprotective agent) [24] [30] were evaluated on murine C2C12 myoblasts. The ability of MTSO to attenuate cell death and oxidative stress induced by 7β-hydroxycholesterol (7β-OHC) was evaluated on C2C12 with a special focus to the effects at the peroxisomal level. The peroxisomes are cytoplasmic organelles often circular in appearance from 0.1 to 1 µm in diameter; they are highly dynamic and move along microtubules [36] [37] [38]. The peroxisomes are present in all cells, except erythrocytes, and their activity is important in the metabolism of lipids (very long chain and branched fatty acids; cholesterol and bile acids; plasmalogens; eicosanoids) and the catabolism of polyamines [39] [40] [41]. The peroxisomes also participate in cellular RedOx balance [42], and several studies suggest that peroxisomal dysfunctions

contribute to ageing [43] [44] [45] and neurodegeneration [46] [47] [48]. In addition, the peroxisomes that results from the import of proteins from the endoplasmic reticulum are closely connected to the mitochondria (involved in normal and pathological ageing) both at the spatial and functional level, and the activities of one strongly influence the activities of the other [49]. It is therefore essential to better understand the peroxisomal modifications induced by 7β-OHC on skeletal muscle by using C2C12 cells as a model in the context of sarcopenia in order to identify natural or synthetic molecules as well as mixtures of molecules (oils) that can prevent peroxisomal dysfunctions. Like mitotherapy, which is a promising approach to prevent neurodegeneration [50], pexotherapy could constitute a new therapeutic axis to address ageing but also to prevent and/or treat age-related diseases. In this context, the identification of natural products associated with the Mediterranean diet, such as MTSO and its major nutrients, offers a lot of opportunities [51] [52]. Our data obtained on C2C12 cells show the ability of MTSO and α-tocopherol to strongly attenuate 7β-OHC-induced cytotoxicity (ROS overproduction and cell death) as well as the associated peroxisomal changes.

2-Material and Methods

2.1-Cell Culture and Treatments

Murine C2C12 myoblasts, which have the ability to differentiate in myotubes in particular culture conditions, were cultured in Dulbecco's modified Eagle's medium (DMEM, Lonza, Amboise, France) containing 10% (v/v) of heat-inactivated fetal bovine serum (FBS) (Pan Biotech, Aidenbach, Germany) and 1% antibiotics (penicillin, streptomycin) (Pan Biotech). The cells were maintained at 37°C in a humidified 5% CO_2 incubator and passaged twice a week. Once 80% confluence was achieved, the cells were seeded either into Petri dishes of 10 cm in diameter (1.2

$\times 10^6$ cells per Petri dish), in six-well plates (2×10^5 cells per well), or in 96-well plates (10×10^4 cells per well). 7β-OHC was either from Sigma-Aldrich or provided by Mohammad Samadi (University of Lorraine, Metz, France); the purity was higher than 98%. The stock solution of 7β-OHC (800 µg/mL = 2 mM) was prepared as previously described [24]. The stock solution of MTSO and PLSO was prepared at 80 mg/mL in dimethyl sulfoxide (DMSO; Sigma-Aldrich). α-tocopherol (Sigma-Aldrich) solution was prepared to 80 mM in absolute ethanol, as previously described [24]. The stock solution of oleic acid (Sigma-Aldrich) was prepared at 50 mM in ethanol as previously described [53], and oleic acid (100 µM) was used as a positive control to induce lipid droplets formation [53]. After 12 h of cell culture, the growth medium was removed and the cells were incubated with 7β-OHC (50 µM) for 24 h with or without MTSO (100 µg/mL), or α-tocopherol (400 µM) (used as a positive control for cytoprotection). The concentrations of 7β-OHC, MTSO, and α-tocopherol as well as the times of treatment were in accordance with our previous study [22].

2.2-Analysis of cell morphology by phase-contrast microscopy

Cell morphology (adherent and non-adherent cells) and cell density was observed and photographed after 24 h of treatment in the absence or presence of 7β-OHC (50 µM) with or without MTSO (100 µg/mL), or α-tocopherol (400 µM), under an inverted phase-contrast microscope (Axiovert 40 CFL, Zeiss, Jena, Germany) equipped with a digital camera (Axiocam lCm1, Zeiss).

2.3-Measurement of cell viability with the Fluorescein Diacetate (FDA) assay

Living C2C12 cells were determined using a lipophilic fluorochrome, fluorescein diacetate (FDA; Sigma-Aldrich). After 24 h of treatment with or without 7β-OHC in the presence or

absence of MTSO, or α-tocopherol, C2C12 cells were incubated in the dark with FDA (15 µg/mL in PBS, 5 min, 37°C) and rinsed with PBS. The fluorescence intensity of the fluorescein ($\lambda_{Ex\ max}$ = 485 nm, $\lambda_{Em\ max}$ = 528 nm) was measured with a Tecan fluorescence microplate reader (Tecan Infinite M200 Pro, Lyon, France). The experiments were realized in triplicate, and the data were expressed as % of control: (Fluorescence (assay) × 100) / Fluorescence (control)).

2.4-Measurement of cell viability with the MTT assay

MTT (3-(4-,5-dimethylthiazol-2-yl)-2,5-diphenyltetrazolium bromide) assay was used to evaluate the effects of MTSO and α-tocopherol on cell viability. This colorimetric assay is based upon the ability to reduce a tetrazolium salt (MTT) and form a blue formazan product by the mitochondrial enzyme succinate dehydrogenase ([54] [55]). Cells were seeded in 96-well plates and treated with different concentrations of MTSO and α-tocopherol for 24 h. At the end of the treatment, cells were incubated with MTT (0.05 mg /·mL) for 3 h in the dark. The formazan crystals formed were solubilized with 200 µL DMSO. The plates were read at 570 nm with a microplate reader (TECAN Sunrise, Tecan, Lyon, France).

2.5-Quantification of adherent cells with the Sulforhodamine 101 (SR101) assay

Sulforhodamine 101 (SR101; Sigma Aldrich) was used to quantify adherent cells by its ability to stain cellular proteins [56]. After 24 h of treatment with or without 7β-OHC in the presence or absence of MTSO, or α-tocopherol, C2C12 cells were fixed with ethanol 70% for 20 min at 4°C. After two washes in PBS, cells were stained with an SR101 solution (1.5 µg/mL, 30 min, and 4°C). Then, the cells were washed twice with PBS and the fluorescence was measured with a fluorescent plate reader (Infinite M200, TECAN) using Ex 535 nm / Em 610 nm. The experiments were realized in triplicate and the data were expressed as % of control.

2.6-Measurement of transmembrane mitochondrial potential (ΔΨm) with $DiOC_6(3)$

The variation in the mitochondrial transmembrane potential (ΔΨm) was detected using 3,3'-dihexyloxacarbocyanine iodide ($DiOC_6(3)$) [24]. After 24 h of treatment, adherent and non-adherent C2C12 cells were pooled, stained with a solution of $DiOC_6(3)$ (Invitrogen/Thermo Fisher Scientific, Montigny le Bretonneux, France) at 40 nM (15 min; 37°C), and analyzed on a BD Accuri™ C6 flow cytometer (BD Biosciences). Mitochondrial depolarization is indicated by a decrease in the green fluorescence intensity collected through a 520 ± 10 nm band-pass filter. For each sample, 10,000 cells were acquired, and data analyses were performed with FlowJo software (Carrboro, NC, USA)).

2.7-Measurement of intracellular ROS with dihydroethidium staining

The production of ROS, including the intracellular superoxide anion ($O_2^{\bullet -}$), was quantified by flow cytometry after staining with dihydroethidium (DHE; Thermo Fisher Scientific). After 24 h of treatment, C2C12 cells (adherent and non-adherent cells) were stained with a 2 µM DHE solution for 15 min at 37°C and then analyzed on a BD Accuri™ C6 flow cytometer. The production of ROS was monitored by oxidized DHE that exhibits an orange/red fluorescence ($\lambda_{Ex\ Max}$ = 488 nm; $\lambda_{Em\ Max}$ = 575 nm) [57]. The fluorescent signals of the DHE-stained cells were collected through a 580 nm band-pass filter. 10,000 cells were acquired for each sample. Data analyses were performed using FlowJo software.

2.8-Microscopical visualization of lipid droplets with Oil Red O (ORO)

Lipid droplets are dynamic organelles and function as a storage structure for neutral lipids, including triglycerides and cholesterol esters [58]. The presence of neutral lipids was investigated

by staining with Oil Red O (ORO; Sigma Aldrich). ORO is soluble in neutral lipids and remains dissolved in triglycerides after washing. To this end, at the end of treatments, C2C12 cells cultured in 6 well-plates were washed with PBS and stained with ORO solution (three parts 0.5% ORO dye in isopropanol into two parts water) for 30 min, and stored in the dark at room temperature [53]. The stained cells were washed three times with water and three contiguous observation fields always taken in the center of a 6-well plate were observed under an inverted phase contrast microscope (Axiovert 40 CFL, Zeiss).

2.9-Determination of the peroxisomal status

2.9.1-Transmission electron microscopy

Transmission electron microscopy was realized as previously described [22] to simultaneously visualize peroxisomal and mitochondrial ultrastructure and morphology in C2C12 cells treated for 24 h with or without 7β-OHC in the presence or absence of MTSO, or α-tocopherol. The sample preparation technique used is specifically adapted to allow the detection of peroxisomes. C2C12 myoblasts (10^6 cells) were fixed for 1 h at 4°C in 2.5% (w/v) glutaraldehyde diluted in a cacodylate buffer (0.1 M, pH 7.4), washed twice in cacodylate buffer, incubated in the dark for 1 h at 21°C in Tris–HCl (0.05 M, pH 9.0) containing diaminobenzidine (DAB: 2.5 mg/mL) and H_2O_2 (10 µL/mL of a 3% solution); washed in cacodylate buffer (0.1 M, pH 7.4) for 5 min at 21°C; post-fixed in 1% (w/v) osmium tetroxide diluted in cacodylate sodium (0.1 M, pH 7.4) for 1 h at 21°C in the dark; and rinsed in cacodylate buffer (0.1 M, pH 7.4). The preparations were dehydrated in graded ethanol solutions and then embedded in Epon. Ultrathin sections were cut with an ultramicrotome, contrasted with uranyl acetate and lead citrate, and examined using an HT7800 electron microscope (Hitachi, Tokyo, Japan).

2.9.2-Apotome evaluation of the level and topography of ABCD3 peroxisomal transporter

ABCD3 peroxisomal transporter was detected by indirect immunofluorescence [59]. Cells were cultured on glass slides in six-well plates. After 24 h of treatment, adherent and non-adherent C2C12 cells were collected, fixed with 2% (w/v) paraformaldehyde for 15 min at room temperature (RT), and rinsed twice with PBS. Cells were permeabilized for 30 min at RT with a PFS buffer (PBS/0.05% saponin/10% FCS). After washing in PBS, cells were incubated (1 h, RT) with an appropriate rabbit polyclonal antibody raised against ABCD3 (# 11523651, Pierce/Thermo Fisher Scientific, Asheville, NC, USA) diluted (1/500) in PFS buffer. Cells were washed and incubated in the dark (30 min, RT) with a goat anti-rabbit 488-Alexa antibody (Santa-Cruz Biotechnology, Santa Cruz, CA, USA) diluted at 1/500 in PFS buffer. After washing in PBS, cells were stained with Hoechst 33342 (1 µg/mL) and then mounted in Dako fluorescent mounting medium (Dako, Copenhagen, Denmark). The slides were stored in the dark at 4°C and examined with structured illumination microscopy (Apotome 2 Imaging System, Zeiss). The images were realized with ZEN imaging software (Zeiss).

2.9.3-Flow cytometric quantification of ABCD3 peroxisomal transporter

For flow cytometric analyses, adherent cells were detached by trypsinization, mixed with non-adherent C2C12 cells, fixed with 2% (w/v) paraformaldehyde diluted in PBS for 15 min at RT and then rinsed twice with PBS. Cells were permeabilized for 30 min at RT with PFS buffer. After washing in PBS, cells were incubated (1 h, RT) with an appropriate rabbit polyclonal antibody raised against ABCD3 (# 11523651, Pierce/Thermo Fisher Scientific) diluted (1/500) in PFS buffer. Cells were washed and incubated in the dark (30 min, RT) with a goat anti-rabbit 488-Alexa antibody (Santa-Cruz Biotechnology) diluted at 1/500 in a PFS buffer. After washing

in PBS, cells were resuspended in PBS and immediately analyzed on a BD Accuri™ C6 flow cytometer (BD Biosciences). The green fluorescence of 488-Alexa was collected with a 520 ± 20 nm band-pass filter. For each sample, 10,000 cells were acquired, and data analyses were performed using FlowJo software.

2.9.4-Quantification by RT-qPCR of gene expression associated with peroxisomal β-oxidation

RNA extraction from myoblasts was performed using the RNeasy Mini Kit (Qiagen, Courtaboeuf, France) according to the manufacturer's instructions. The purity of each mRNA sample was controlled by the ratio of absorbance at 260 nm and 280 nm (ratios of 1.8 - 2.2 were considered satisfactory). 1 µg of total mRNA from each sample was converted into single-stranded cDNA using the iScript cDNA Synthesis kit (BioRad, Marne la Coquette, France) according to the following procedure: 5 min at 25°C, 20 min at 46°C, and 5 min at 95°C. cDNA was then amplified using Takyon TM Rox SYBR Master Mix dTTP Blue (Eurogentec, Liège, Belgium) and specific forward and reverse primers. The following primers were used:

- *Abcd3*: forward 5′-ctgggcgtgaaatgactagattg-3′ and reverse 5′-cttctcctgttgtgacaccattg-3′
- *Pex 5*: forward 5′-gtgggcagcagagtttatacag-3′ and reverse 5′-ctccctcctcaagtcgatgc-3′
- *Pex13*: forward 5′-aaccaacacttacaagagtgcc-3′ and reverse 5′-ccgtaggctccatatccagaag-3′
- *Pex14*: forward 5′-acagcagtgaagttcctacaga-3′ and reverse 5′-gccaggtcaatctcttcgtct-3′

Thermal cycling conditions were as follows: activation of DNA polymerase (95°C, 10 min), followed by 40 cycles of amplification at 95°C for 15 s, 60°C for 30 s, and 72°C for 30 s,

followed by a melting curve analysis to control for the absence of nonspecific products. Gene expression was quantified using cycle to threshold (Ct) values and normalized by the *36B4* reference gene (forward 5′-gcgacctggaagtccaacta-3′ and reverse 5′-atctgcttggagcccacat-3′). The quantitative expression of *Abcd3*, *Pex5*, *Pex13*, and *Pex14* was determined as fold induction of the control.

2.9.5-Characterization and quantification of ABCD3, ACOX1, and MFP2 peroxisomal proteins by western blotting

After 24 h of treatment, C2C12 cells were trypsinized, washed with PBS, harvested, and lysed in a RIPA buffer (10 mM Tris-HCl, pH 7.2, 150 mM NaCl, 0.5% Nonidet NP40, 0.5% Na deoxycholate, 0.1% SDS, 2 mM EDTA and 50 mM NaF) containing a complete protease inhibitor cocktail (Roche Diagnostics, Indianapolis, IN, USA) diluted 1/25 for 30 min on ice. After centrifugation at 20,000 g for 20 min at 4°C, the total protein concentration of supernatant was measured using bicinchoninic acid reagent as a standard (Sigma Aldrich). 70 µg of protein were separated on a 14%, 12%, or 8% SDS-PAGE gel and blotted onto a PVDF membrane (Bio-Rad). After blocking non-specific binding sites with 5% milk powder in PBST (PBS, 0.1% Tween 20, pH 7.2) for 1 h, membranes were incubated overnight (4°C) with the primary antibody diluted in 5% milk PBST. The peroxisomal β-oxidation was evaluated by using the following rabbit polyclonal antibodies: anti-ABCD3 1/500 (#11523651, Pierce/Thermo Fisher Scientific), anti-multifunctional enzyme type 2 (MFP2) 1/1000 (#GTX114978, Gentex/Euromedex, Souffelweyersheim, France), and anti-ACOX1 1/200 (rabbit polyclonal antibody) detecting the three ACOX1 isoforms at 75, 50, and 25 kDa [60]. An antibody directed against β-actin (A2228; mouse monoclonal antibody; Sigma-Aldrich) was used at a final concentration of 1/10,000. The

membranes were washed three 5 min with PBST and incubated with a secondary horseradish peroxidase-conjugated goat anti-rabbit antibody (#7074; Cell Signaling) or an anti-mouse antibody (#sc-2005, Santa-Cruz Biotechnology) diluted at 1/5,000 in 1% milk powder in PBST. The membranes were then washed, and antibody binding was revealed using an enhanced chemiluminescence detection kit (Supersignal West Femto Maximum Sensitivity Substrate, Thermo Fisher Scientific) and a Chemidoc XRS+ (Bio-Rad). The levels of ABCD3, ACOX1, and MFP2 were determined versus β-actin and were calculated with Image Lab software (Bio-Rad).

2.9.6-Characterization and quantification of very-long-chain fatty acids (VLCFA) by gas chromatography coupled with mass spectrometry (GC / MS)

Fatty acids, including very-long-chain fatty acids (VLCFA; C ≥ 22) [61], were analyzed using GC/MS as previously described by Blondelle et al. [62]. Total cellular lipids were extracted by Folch's method [63]. Fatty acids were quantitated with the use of an internal standard (C19:0), and calibration curves were obtained with fatty acid authentic standards.

2.10-Mass spectrometry analysis of sterols

Cellular homogenates were added to a screw-capped vial sealed with a teflon septum together with deuterium labeled or structural homologous internal standards, butylated hydroxytoluene and EDTA and flushed with argon for 20 min to remove air. Alkaline hydrolysis was allowed to proceed at room temperature (22°C) with magnetic stirring for 30 min in the presence of ethanolic 0.5 M potassium hydroxide solution. Sterols and oxysterols were collected by liquid to liquid extraction with hexane. Oxysterols were purified by SPE separation [64]. After correction

of pH (<3) with HCl, all metabolites were extracted in sequential liquid to liquid extraction with hexane and ethylacetate. The organic solvents were evaporated under a gentle stream of argon and converted into trimethylsilyl ethers with [N,O-Bis(trimethylsilyl)trifluoroacetamide] (BSTFA) with trimethylchlorosilane (TCS) 1% (Pierce / Thermo Fisher Scientific). GC–MS analysis was performed as previously described [65].

2.11-Statistical Analysis

Statistical analyses were performed using GraphPad Prism 8.0 software (GraphPad Software, San Diego, CA, USA). Data were represented as the mean ± standard deviation (SD) and compared either with a Student's t-test or with an ANOVA test followed by a Tukey's test, which allows multiple comparisons and permits to assess any interaction. The heatmap representation was realized with GraphPad Prism 8.0 software. Data were considered statistically significant at a value of $p \leq 0.05$.

3-Results

3.1-Phytochemical profile of milk thistle seed oil (MTSO)

The MTSO used was from a Tunisian region (Sousse). It was prepared as previously described [29] and its phytochemical profile was established by Zarrouk et al. [30]. The main characteristics of MTSO, which is a Mediterranean oil containing an elevated level of α-tocopherol, are summarized in **Table 1**.

3.2-Attenuation of 7β-hydroxycholesterol-induced cell death by MTSO and α-tocopherol on C2C12 cells

The impact of MTSO on cell growth, transmembrane mitochondrial potential (ΔΨm), and ROS production were evaluated on 7β-OHC-treated C2C12 cells. To this end, C2C12 cells were cultured with or without 7β-OHC (50 µM) in the presence or absence of MTSO (100 µg/mL) or α-tocopherol (400 µM) and then stained either with fluorescein diacetate (FDA), sulforhodamine 101 (SR101), 3,3'-dihexyloxacarbocyanine iodide ($DiOC_6(3)$) or dihydroethidium (DHE). The concentration of 7β-OHC used corresponds to the 50% inhibiting concentration (IC50); it inhibits by 50% the viability of C2C12 cells (**Supplementary S1A**). Concentrations of MTSO and α-tocopherol used significantly increase the viability of C2C12 cells (**Supplementary S1B and S1C**). In addition, it has also previously been shown on 158N murine oligodendrocytes i) that the concentration of 400 µM was the highest non-cytotoxic concentration of α-tocopherol and ii) that this latter, compared to lower concentrations, was the most efficient to counteract 7β-OHC- and 7KC-induced cell death [24].

With the FDA and SR101 assays, a marked decrease in cell viability and density was observed under treatment with 7β-OHC compared to control and vehicle (ETOH and/or DMSO)-treated cells. Comparatively to untreated cells, the cytotoxic effects of 7β-OHC were characterized by a lower percentage of FDA-positive cells (cells with altered plasma membrane) and a lower percentage of SR101-positive cells (lower number of adherent cells) (**Figure 1A-B)**, whereas no significant differences were observed between untreated cells (control), vehicle-treated cells, MTSO-, and α-tocopherol-treated cells (**Figure 1A-B**). These cytotoxic effects were strongly and significantly attenuated with MTSO and α-tocopherol (**Figure 1A-B**), indicating that MTSO and α-tocopherol provided cytoprotection against 7β-OHC induced-cell death which is associated with a loss of cell adhesion as shown by the presence of round cells floating in the culture

medium by phase-contrast microscopy (**Supplementary Figure S2)**. In addition, by phase microscopy, no difference was observed between control, vehicle-treated cells, MTSO-, and α-tocopherol-treated cells: the cell density and morphology were similar (**Supplementary Figure S2**). This cytoprotective effect of MTSO and α-tocopherol could be due at least in part to the ability of MTSO and α-tocopherol to reduce the cellular accumulation 7β-OHC in C2C12 cells from around 25% and 50%, respectively (**Table 2**). As MTSO contains high levels of fatty acids [30], mainly oleic acid, which can favor lipid droplets formation with cytoprotective activities against 7-ketocholesterol (7KC) – induced oxidative stress and cell death [53], the ability of MTSO and α-tocopherol to trigger lipid droplets formation was determined after staining with Oil Red O (ORO). Under our different conditions of treatments, no lipid droplets were observed in control, vehicle-treated cells and α-tocopherol-treated cells as well as in MTSO-, (7β-OHC + MTSO)-, and (7β-OHC + α-tocopherol) treated cells whereas around 10% of ORO positive cells were detected in 7β-OHC-treated cells. (**Supplementary Figure S3**).

In addition, after staining with $DiOC_6(3)$, used to measure ΔΨm, a significant increase in C2C12 cells with depolarized mitochondria ($DiOC_6(3)$ negative cells) was observed under treatment with 7β-OHC. Interestingly, MTSO and α-tocopherol strongly prevent the loss of ΔΨm, as shown by lower percentages of cells with depolarized mitochondria (**Figure 1C**). Similar percentages of cells with depolarized mitochondria (in the range of 10%) were observed in control, vehicle-treated cells, MTSO-, and α-tocopherol-treated cells (**Figure 1C**).

After staining with DHE, a strong increase in intracellular ROS level (DHE positive cells) was observed in the presence of 7β-OHC (**Figure 1D**). This percentage of DHE positive cells was significantly attenuated by MTSO and α-tocopherol (**Figure 1D**)**.** Similar percentages of DHE positive cells (in the range of 5%) were observed in control, vehicle-treated cells, MTSO-, and α-tocopherol-treated cells (**Figure 1D**).

3.3-Prevention of 7β-hydroxycholesterol-induced peroxisomal changes by MTSO and α-tocopherol on C2C12 cells

Peroxisomes are key metabolic organelles that participate in the control of RedOx homeostasis and lipid metabolism [66] [67]. There are functionally connected to mitochondria and endoplasmic reticulum; peroxisomes located in the vicinity of mitochondria are often observed [68]. It is therefore supposed that peroxisomal changes (including morphologic, topographic and functional modifications) could favor mitochondrial dysfunctions contributing to the cytotoxic activities of 7β-OHC on C2C12 cells. Therefore, several peroxisomal parameters were studied with the use of complementary methods: transmission electron microscopy, fluorescence microscopy (Apotome) and flow cytometry, western blotting, RT-qPCR, and GC / MS.

Under standard electron microscopy conditions all organelles are visualized except peroxisomes. However, under our particular staining conditions of cell samples with diaminobenzidine, all organelles (including peroxisomes) can be simultaneously visualized [59]. Thus, the observations of C2C12 cells by transmission electron microscopy allowed us to simultaneously reveal essential cellular constituents, namely peroxisomes, mitochondria, and endoplasmic reticulum. Control cells, MTSO (100 µg/mL)- and α-tocopherol (400 µM)- treated cells have morphologically normal mitochondria with numerous cristae, round peroxisomes that are homogeneous in size (in the range of 0.4 ± 0.1 µm) and an endoplasmic reticulum (ER) which is rich in ribosomes and easily identified (**Figure 2A, C and E**). In the presence of 7β-OHC (50 µM), major changes in the size and shape of the mitochondria and peroxisomes were detected. Several peroxisomes were observed in numerous cytoplasmic vacuoles, evocating a pexophagy process, and some elongated mitochondria were present **(Figure 2B)**. These changes were

attenuated by MTSO and α-tocopherol treatment: the number of vacuoles containing peroxisomes was decreased whereas the number of morphologically normal mitochondria was increased (**Figure 2D and F**).

Moreover, the peroxisomal transporter ABCD3 is considered as a good marker for assessing peroxisomal mass and may also provide information on peroxisome biogenesis ([69]). After staining with an anti-ABCD3 polyclonal antibody, stacks of structured illumination microscopy images obtained in untreated cells, MTSO-, and α-tocopherol-treated cells showed a high density and a homogeneous distribution of peroxisomes in the cytoplasm (**Figure 3A**). After incubation with 7β-OHC, a marked decrease in peroxisomal density, as well as peroxisomal aggregates (which could correspond to pexophagy vesicles), were seen. In the presence of MTSO and α-tocopherol, these peroxisomal changes were attenuated **(Figure 3A)**. By flow cytometry, in agreement with the observations made by fluorescence microscopy (Apotome), a significant increase in the percentage of cells with ABCD3 reduced level (in the range of 50%), indicating a decrease of the peroxisomal mass, was observed (**Figures 3B-C**). Interestingly, this decrease of peroxisomal mass induced by 7β-OHC was strongly counteracted in the presence of MTSO and α-tocopherol (**Figures 3A-C**). Indeed, the percentage of cells with reduced ABCD3 level was in the range of 25% and of 20% when 7β-OHC was associated with MTSO and α-tocopherol, respectively (**Figures 3B-C**). Comparatively to untreated cells, no effects of vehicles (ETOH, DMSO), MTSO, and α-tocopherol were observed on the peroxisomal mass: the percentages of cells with reduced ABCD3 were similar (around 20%) in these different conditions (**Figure 3B-C**). In addition, RT-qPCR was applied to quantify *Abcd3* gene expression levels. In the presence of MTSO (100 µg/mL) or α-tocopherol (400 µM), no differences in the mRNA expression level of *Abcd3* was observed compared to untreated, MTSO, α-tocopherol, and vehicle-treated cells. However, with 7β-OHC, the mRNA expression level of *Abcd3* gene was significantly decreased

(**Figure 3D**). The association of MTSO or α-tocopherol with 7β-OHC counteracted this decrease (**Figure 3D**). Noteworthy, the results obtained by RT-qPCR agreed with those of western blot analysis (**Figure 4**).

In order to precise the impact of 7β-OHC on peroxisomal biogenesis the expression and level of peroxins, including Pex5, Pex13, and Pex14, were studied. Pex5 transports newly synthesized proteins from the cytosol to the peroxisomal matrix [70]. Pex13 and Pex14 are key components of the peroxisomal docking complex localized at the peroxisomal membrane level and are required for peroxisome formation [71]. As shown by RT-qPCR, a significant decrease in *Pex5* mRNA level was observed in 7β-OHC-treated cells compared to control, MTSO-, and α-tocopherol-treated cells (**Figure 3E**). However, in the presence of 7β-OHC, an increase in *Pex13* and *Pex14* mRNA levels were observed (**Supplementary Figure S4**) underlying that peroxin expressions are differentially regulated under treatment with 7β-OHC.

In addition, the effect of 7β-OHC on peroxisomal β-oxidation, which allows the degradation of very-long-chain fatty acids (VLCFA, C≥22), was also studied (**Figure 4A**). This pathway involves Acyl-CoA Oxidase 1 (ACOX1) and the multifunctional protein 2 (MFP2). As shown by Western blot, significant decreases in ACOX1 (isoforms 75, 50, and 25 kDa) and MFP2 occurred in the presence of 7β-OHC (**Figure 4B**). When MTSO or α-tocopherol were associated with 7β-OHC, these decreases were strongly and significantly attenuated (**Figure 4B**). As 7β-OHC induces a decreased level of ACOX1 and MFP2 involved in peroxisomal β-oxidation (**Figures 4A-B**), this effect should favor the accumulation of VLCFA, which can contribute to cellular dysfunctions (oxidative stress and cell death induction) [72] [73]. Therefore, the intracellular level of VLCFA was determined by GC / MS in our different culture conditions. As shown in **Figure 5**, the analysis of VLCFA revealed a significant increase in behenic acid (C22:0),

lignoceric acid (C24:0), nervonic acid (C24:1 n-9), cerotic acid (C26:0), and hexacosenoic acid (C26:1 n-9) levels, following treatment with 7β-OHC. This increase was normalized when 7β-OHC-treated C2C12 cells were simultaneously exposed to MTSO or α-tocopherol (**Figure 5**).

Altogether, our findings demonstrate that 7β-OHC-induced several peroxisomal changes i) which impact peroxisomal topography and mass, biogenesis, as well as β-oxidation and ii) which are strongly attenuated by MTSO and α-tocopherol. These data are summarized in the heatmap presented in **Figure 6**.

4-Discussion

The oxysterols, formed either by auto-oxidation of cholesterol or enzymatically or by both processes, have a wide range of biological activities [74] and some of them are cytotoxic both *in vitro* and *in vivo* [11]. This is the case of 7β-OHC, which is a pro-oxidant and pro-inflammatory molecule [14]. Moreover, 7β-OHC can also activate different types of cell death: apoptosis, autophagy, necrosis, and oxiapoptophagy [14] [35] [75]. Depending on the cell type considered, the ability of 7β-OHC to induce ferroptosis cannot be excluded [76]. Given its characteristics and the high levels of 7β-OHC observed in biological fluids and lesions of certain age-related diseases (vascular wall in the case of cardiovascular diseases; cerebral cortex in the case of Alzheimer's disease) [14], it seems that 7β-OHC likely contributes to the pathophysiology of these diseases and is also involved in ageing [17] [77] [78]. Recently, we have also shown that 7β-OHC was significantly increased (student's t-test; $p < 0.05$) in the plasma of normocholesterolemic patients aged 65 and over suffering from sarcopenia (7β-OHC plasma level: non sarcopenic subjects: 0.5 to 4 nM, 2.12 ± 0.61 nM; sarcopenic patients: 1 to 7 nM, 3.29 ± 1.28 nM), characterized by a loss of muscle mass and strength, which is a factor of frailty in the

elderly [22]. The plasma level of 7β-OHC + 7KC, which can be converted in 7β-OHC [14], was also significantly increased (student's t-test; $p < 0.05$) in the same subjects (7β-OHC + 7KC: non sarcopenic subjects: 3 to 13 nM, 7.66 ± 2.62 nM; sarcopenic patients: 7 to 30 nM, 12.65 ± 4.50 nM) [22]. In addition, on C2C12 cells differentiated into myotubes, we observed that the toxicity of 7β-OHC was greater than that of 7KC (our data not shown). Altogether, these data led us to choose C2C12 murine myoblasts as a cell model to demonstrate the strong cytotoxic activity of 7β-OHC [22]. To this end, 7β-OHC was used at its IC50 value (50 µM). Although this IC50 is elevated in the context of sarcopenia, while it is physiologically acceptable for cardiovascular diseases and Alzheimer's disease [15], the concentration of 7β-OHC used on C2C12 makes it possible to compare the effects of this oxysterol from one cell type to another by addressing under well-defined conditions the effects of 7β-OHC on organelles, oxidative stress and cell death [14]. Thus, on C2C12 cells, the effects of 7β-OHC were characterized by an induction of oxidative stress, alterations of organelles (mitochondria, peroxisome), and induction of cell death [22]. The observed cytotoxicity was strongly mitigated by Tunisian *Pistacia lentiscus* L. seed oil (PLSO), rich in antioxidants and widely used in traditional Tunisian cooking [22]. Another Mediterranean oil used both in Tunisian cuisine and in traditional medicine is milk thistle seed oil (MTSO) [79]. In the present study, we are particularly interested in the effects of MTSO from the Sousse region (Tunisia) [30]. Given that 7β-OHC-induced mitochondrial dysfunctions are quite well described both morphologically and functionally on different cell types [80], and as mitochondria and peroxisomes are functionally connected organelles, we focused on the characterization of 7β-OHC-induced peroxisomal changes [81]. Indeed, mitochondrial dysfunction can favor peroxisomal dysfunction and reciprocally [49]. In the present study, we show that MTSO, enriched with α-tocopherol [30], strongly attenuates 7β-OHC-induced cell death on C2C12 cells. In addition, we are particularly interested in the ability of this oil to correct

the peroxisomal alterations induced by 7β-OHC. We show that MTSO prevents peroxisomal topographical, morphological and functional changes induced by 7β-OHC as efficiently as α-tocopherol (one of the most potent lipid-soluble antioxidants in the body) [82], employed at high concentration (400 μM) often used as a cytoprotective molecule to attenuate the deleterious effects of cytotoxic oxysterols including 7-ketocholesterol (7KC), 7β-OHC and 24S-hydroxycholesterol [14] [24] [26].

On C2C12 myoblasts, 7β-OHC (50 μM, 24 h) is a toxic compound that triggers a mode of cell death associated with ROS overproduction. It is well established that this overproduction is partly mitochondrial [22]. However, in the presence of 7β-OHC, as observed with 7KC, an activation of NADP(H) oxidase cannot be excluded [83]. In addition, peroxisomal dysfunctions could also contribute to the increase in ROS production. Indeed, on C2C12 cells, 7β-OHC induce a decrease of *Abcd1* and *Acox1* mRNA levels. It has been also shown on 158N murine oligodendrocytes that decreasing *Abcd1* and *Acox1* expression with siRNAs increases ROS production [73]. As the overproduction of ROS is known to promote inflammation [84], it is hypothesized that the ability of 7β-OHC to trigger mitochondrial and peroxisomal dysfunctions leading to a rupture of RedOx homeostasis could favor the increase of pro-inflammatory cytokines often observed in patients with severe forms of sarcopenia [85].

On C2C12 cells, the 7β-OHC-induced oxidative stress is associated with a mode of cell death characterized by important morphological changes as revealed by phase-contrast microscopy and TEM. As previously reported on 7β-OHC-treated adherent cells, 7β-OHC-induced cell death is associated with a reduced number of adherent cells and an increased number of cells floating in the culture medium [14] [80]. As oxysterols, including 7β-OHC, have an important impact on the biophysical properties of the plasma membrane, including the formation of liquid-ordered

domains, this could at least in part contribute to the loss of cell adhesion [86]. In this context, deleterious effects of 7β-OHC on the biophysical properties of organelle membranes (mitochondria, peroxisome) are also very likely. It has been previously shown by video microscopy on A7r5 rat smooth muscle cells, that this loss of cell adhesion was preceded by the drop of ΔΨm analyzed with the use of $DiOC_6(3)$ [87]. By analogy, the important mitochondrial changes triggered by 7β-OHC on C2C12 cells, especially the loss of ΔΨm, could contribute to this process. Note that this functional change is also associated with ultrastructural modifications of mitochondria revealed by the presence of swollen and large mitochondria also observed on other cell types, such as 158N murine oligodendrocytes, in the presence of toxic oxysterols such as 7β-OHC [88]. It is suggested that these modifications aimed to increase the surface area of the mitochondrial cristae, which are the site of oxidative phosphorylation for ATP production [89]. These ultrastructural modifications could thus be considered as a cellular response to mitigate mitochondrial energy dysfunctions and to prevent cell death and major peroxisomal activities requiring ATP production, such as the transport of various types of fatty acids (VLCFA, docosahexahenoic acid (C22:6 n-3), pristanic acid, di- and trihydroxy-cholestanoic acid (DHCA and THCA), and dicarboxylic acid (DCA)) in the peroxisome via ATP binding cassette transporter subtype D (ABCD1, ABCD2, and ABCD3), whose activity requires ATP [90].

If we consider that ROS overproduction and mitochondrial dysfunctions can have several consequences on the peroxisomal status and subsequently on the activity of skeletal muscle cells, other modifications, independent of these parameters are also to be envisaged. This has led to the clarification of 7β-OHC effects not only on peroxisomal β-oxidation but also on peroxisomal mass, topography, and ultrastructure. To date, little is known on the role of peroxisomes in skeletal muscle cells in normal and pathological conditions. However, in patients with congenital

peroxisomopathies (adrenomyeloneuropathies, Refsum disease), skeletal muscle damages have been reported and are characterized by exercise intolerance and myalgia suggesting that peroxisomal abnormalities affect muscle function [91]. With the different complementary parameters considered in this study to evaluate the effects of 7β-OHC on this organelle, it emerges that 7β-OHC (as shown with 7KC on 158N murine oligodendrocytes [92] [93], BV-2 microglial cells [94] and N2a neuronal cells [95]) induces several and important peroxisomal modifications. Therefore, in several age-related diseases (cardiovascular diseases, Alzheimer's disease, age-related macular degeneration, cataract, sarcopenia), where increased levels in 7β-OHC and/or 7KC are often observed in the organs affected by the disease but also in the biological fluids (plasma and/or cerebrospinal fluid), peroxisomal alterations are likely to occur. It was therefore of interest to analyze and characterize the effects of 7β-OHC at the peroxisomal level using C2C12 cells as cell model. Interestingly, 7β-OHC level is increased in the plasma of sarcopenic patients [22]. Therefore, it is also important to find molecules or mixtures of molecules able to counteract these peroxisomal modifications leading to peroxisomal dysfunctions: this is the purpose of pexotherapy.

From an ultrastructural point of view, the results on 7β-OHC-treated C2C12 myoblasts evoke those obtained on 158N oligodendrocytes when these latter were cultured with either 7β-OHC or 7KC [80]: the peroxisomes are heterogeneous in morphology and size and are often present in vacuoles whose number is increased compared to untreated cells. In highly specialized hospital pathology laboratories, these peroxisomal ultrastructural changes could serve as biomarkers of oxysterol toxicity in tissues of different organs. Electron microscopy (in the absence of molecular biomarkers that can be used routinely) could exceptionally be a tool to consolidate a pathophysiological hypothesis to address peroxisomal alterations. The presence of vacuoles

containing altered peroxisomes suggests a process of pexophagy as demonstrated in 7KC-treated 158N cells [93]. This hypothesis is supported by the decrease in peroxisomal mass quantified by flow cytometry using ABCD as a peroxisomal mass marker [59] [69] [94]. Furthermore, by RT-qPCR, a decrease in the *Abcd3* mRNA level is also observed. The decrease in peroxisomal mass and the morphological alterations observed are also associated with a reduction of the expression of the gene encoding for the Pex5 protein, involved in peroxisomal biogenesis: Pex5 acts as a shuttle for the import of peroxisomal matrix proteins [70]. Altogether, our data support that the decrease in peroxisomal mass in 7β-OHC- treated C2C12 cells could be the consequence of an induction of pexophagy and a decrease in peroxisomal biogenesis. As a decreased Pex5 level has been described during ageing in cortical neurons in male and female mouse brains [96], our data suggest that 7β-OHC could also affect ageing in myoblasts. On the other hand, in the presence of 7β-OHC, we also observed an increase in the mRNAs of two peroxins, Pex13 and Pex14, which are also involved in peroxisomal biogenesis [71] and are often deficient in Zellweger's disease, a rare and fatal peroxisomopathy [97]. However, it has been described that Pex14 can contribute to autophagy [98]. Pex14 could therefore favor pexophagy that can be induced by 7β-OHC. Similarly, the peroxin Pex13 was involved in peroxisomal biogenesis and has been associated to the activation of selective autophagy of Sindbis virus (virophagy) and to autophagy of altered mitochondria (mitophagy) [99]. Thus, under the effect of 7β-OHC, the activation of a mitophagy process involving Pex13 could be explained at least in part by the fact that this oxysterol induces several mitochondrial dysfunctions.

Furthermore, at the peroxisomal level, western blot analyses showed a decrease in the expression of the peroxisomal enzymes; ACOX1 and MFP2, involved in the peroxisomal β-oxidation of VLCFA [39]. Such results were also observed with 7β-OHC on 158N cells as well as in the

presence of 7KC on 158N, BV-2, and N2a cells [80]. This decrease in the expression of ACOX1 and MFP2 results in a decrease in peroxisomal β-oxidation which favors an intracellular accumulation of VLCFA that can contribute to the lipotoxicity induced by 7β-OHC: activation of oxidative stress and induction of cell death [100]. It is proposed that intracellular accumulation of VLCFA could be a common metabolic biomarker for cytotoxic oxysterols in different cell types.

According to the results obtained with 7β-OHC on C2C12 myoblasts, but also on other types of cells (vascular wall cells, monocytes/macrophages, nerve cells), the prevention of this oxysterol toxicity is always associated with a strong attenuation of oxidative stress and mitochondrial dysfunction [14] [80]. According to the few studies carried out to date, mainly in our laboratory on 158N and C2C12 cells, natural molecules (α-tocopherol; docosahexaenoic acid (DHA); biotin) or synthetic molecules (dimethyl fumarate (DMF); monomethyl fumarate (MMF)) as well as *Pistacia lentiscus* L. seed oil (PLSO), which strongly attenuate 7β-OHC-induced cell death, also prevent the peroxisomal changes induced by this oxysterol [80]. These different molecules are therefore of interest not only in mitotherapy but also in pexotherapy. The present study carried out on C2C12 cells, also shows that MTSO, which strongly reduces the overproduction of ROS, the drop of ΔΨm and cell death on C2C12 cells also strongly counteract peroxisomal alterations. Thus, to date, our data establish that two Mediterranean oils characterized by their strong antioxidant power, MTSO and PLSO, are able to reduce the toxicity of 7β-OHC on vascular, nerve and muscle cells. From a nutritional point of view, these oils, which are rich in α-tocopherol [30], are of potential interest to prevent and/or slow down the development of frequent age-related diseases: cardiovascular and neurodegenerative diseases and sarcopenia. Based on the results presented in this study (Table 1) and described above by Zarrouk et al. [30], and those previously described by Ghzaiel et al. for PLSO [22], the concentrations of α-tocopherol

provided by the MTSO and PLSO in the culture medium are 44 and 15 nmoles / L, respectively. It is therefore unlikely that cytoprotection could be due to α-tocopherol. It is however important to note that the cytoprotective effects observed with MTSO as well as PLSO are similar and are comparable to α-tocopherol, used at high concentration (400 µM) to serve as a reference cytoprotective molecule. Therefore, other molecules with potential cytoprotective activities must be taken in consideration and synergic activities between these molecules (fatty acids, polyphenols, tocopherols) must be considered because of the ability of these compounds to act simultaneously on several signaling pathways involved in 7β-OHC toxicity [80]. Among polyphenols, vanillin is the only one identified in MTSO, however, its low level (3.30 ± 0.01 mg equivalent of quercetin / kg of oil) does not allow to envisage a cytoprotective activity under our experimental conditions. As for phytosterols mainly present in MTSO (β-sitosterol>campesterol>schotenol>stigmasterol>Δ5 avenasterol), no data are available concerning their in vitro cytoprotective effects. Since fatty acids, especially oleic acid, are main compounds of MTSO but also PLSO [22] [30], assessing their ability to prevent oxysterols-induced cell death is a major point. As it has been previously shown that oleic acid has a cytoprotective activity against 7-KC [53], this could be also the case against 7β-OHC. It is therefore hypothesized that the cytoprotection observed with MTSO as well as PLSO could be the consequence of an esterification with oleic acid on the carbon 3 of 7KC and 7β-OHC [32]. This hypothesis could explain similar cytoprotective activities with MTSO and PLSO. In addition, as oleic acid induces the formation of lipid droplets on murine microglial BV-2 cells [53] and as lipid droplets can reduce oxidative stress and lipotoxicity [101] [102], it was important to determine wether MTSO, which is rich in oleic acid, was able to induce lipid droplet formation. The hypothesis of a cytoprotective effect of MTSO, as well as α-tocopherol, involving lipid droplets formation is excluded since no ORO-positive droplets were observed in our different culture conditions except

in the presence of oleic acid used as positive control and 7β-OHC-treated cells. With cytotoxic oxysterols, 24S-OHC, 25-hydroxycholesterol [26], and 7KC [103], which also modifies the ratio (polar lipids/neutral lipids) [104] [105], the presence of lipid droplets has previously been reported. Therefore, with cytotoxic oxysterols, including 7β-OHC, the presence of lipid droplets could be considered as a response to oxidative stress. According to our result, the absence of lipid droplets with MTSO is a positive point. Indeed, a cytoprotection with lipid compounds that do not lead to the formation of lipid droplets is unlikely to lead in vivo to undesirable steatosis in different cell types. In addition, whereas MTSO and PLSO have several common points in terms of cytoprotective activities [22], we also have observed that PLSO more efficiently decreases the cellular accumulation of 7β-OHC than MTSO. It can therefore be assumed that in long term treatments required to prevent the development of age-related diseases associated with increased levels of 7β-OHC and/or 7KC, the cytoprotective efficacy of PLSO could be greater than that of MTSO.

5-Conclusion

In nerve cells (glial, microglial and neuronal cells), it was previously reported that 7β-OHC as well as 7KC induce quantitative and qualitative peroxisomal modifications [106]. In the present study, on C2C12 cells, we demonstrated that 7β-OHC-induced cell death is also associated with important morphological, topographical and functional modifications of peroxisome These effects are strongly attenuated by MTSO as well as by α-tocopherol. The ability of both MTSO and *Pistacia lentiscus* L. seed oil (PLSO) to counteract both peroxisomal and mitochondrial dysfunctions shows that the concept of pexotherapy and mitotherapy can be applied in nutrition

with foods, such as oils from plant seeds used in herbal medicine. In a therapeutic context focused on pexotherapy, the bioavailability and the efficiency of the beneficial compounds present in MTSO could be improved using different approaches. This can include microencapsulation strategies, nano-emulsions, functionalized nanoparticles, chimeric trackable molecules allowing to target specific cell compartments as well as organelles (mitochondria or peroxisome) with specifically designed nanoplatforms associated with cytoprotective compounds present in MTSO (Targeted Organelle Nano-therapy [TORN-therapy]) [107] [108] as well as functional foods. Thus, beyond sarcopenia, the use of MTSO and its major nutrients opens new perspectives for the prevention and / or treatment of diseases, such as age-related diseases, in which alterations of the peroxisome can be involved.

Declaration of Competing Interest

The authors declare no conflict of interest.

Acknowledgements

The authors would like to thank Emmanuelle Prost-Camus and Michel Prost for polyphenols analysis (Laboratoire LARA-Spiral, Couternon, France) as well as Franck Ménétrier (Centre des Sciences du Goût et de l'Alimentation, AgroSup Dijon, CNRS, INRAE, Université Bourgogne Franche-Comté) and Laure Avoscan (Agroécologie, AgroSup Dijon, CNRS, INRAE, University Bourgogne Franche-Comté, Plateforme DimaCell) for their major contribution in transmission electron microscopy. The authors also thank Prof. Hervé Alexandre (Institut Universitaire de la Vigne et du Vin, Université de Bourgogne, Dijon, France) for providing the flow cytometer. The present work was presented in part in an oral communication during the 10th ENOR symposium (web meeting, 16–17 September 2021) (https://www.oxysterols.net/). Imen Ghzaiel also received

financial support from ABASIM (Association Bourguignonne pour les Applications des Sciences de l'Information en Médecine ; Dijon, France). This work was also funded by the Université de Bourgogne (Dijon, France), University of Monastir (Monastir, Tunisia) and the University Tunis El Manar (Tunis, Tunisia).

Figure legends

Figure 1. Cytoprotective effect of milk thistle seed oil (MTSO, *Sylibum marianum*) and α-tocopherol on 7β-hydroxycholesterol-induced cell death, loss of transmembrane mitochondrial potential (ΔΨm), and reactive oxygen species (ROS) overproduction on C2C12 cells. C2C12 cells were incubated for 24 h with or without 7β-OHC (50 µM) in the presence or absence of MTSO (100 µg/mL) or α-tocopherol (α-toco, 400 µM). Under these conditions, cell viability and cell density were determined with the fluorescein diacetate (FDA) and sulforhodamine 101 (SR101) assays, respectively (**A-B**). Loss of transmembrane mitochondrial potential (ΔΨm) was measured by flow cytometry after staining with $DiOC_6(3)$ and evaluated by the percentage of $DiOC_6(3)$ negative cells (**C**). ROS overproduction was measured by flow cytometry after staining with dihydroethidine (DHE) and evaluated by the percentage of DHE positive cells. Data are the mean ± SD of two independent experiments performed in triplicate. A multiple comparative analysis between the groups, considering the interactions, was carried out using an ANOVA test followed by a Tukey's test. A p-value less than 0.05 was considered statistically significant. The statistically significant differences between the groups, which are indicated by different letters, consider the vehicle used. **a**: comparison versus control; **b**: comparison versus ETOH (0.5%); **c**: comparison versus DMSO (0.125%); **d**: comparison versus ETOH (0.1%); **e**: comparison versus (ETOH (0.1%) + DMSO (0.125%)); **f**: comparison versus α-toco (400 µM); **g**: comparison versus MTSO (100 µg/mL); **h**: comparison versus 7β-OHC (50 µM); **i**: comparison versus (7β-OHC (50 µM) + α-toco (400 µM)). No significant differences were observed between the untreated (control) and vehicle-treated cells: EtOH (0.5%), DMSO (0.125%), EtOH (0.1%), and (EtOH (0.1%) + DMSO (0.125%)).

Figure 2. Transmission electron microscopy: ultrastructural characterization of peroxisomes, mitochondria and endoplasmic reticulum on C2C12 cells cultured with or without 7β-hydroxycholesterol in the presence or absence of milk thistle seed oil (MTSO) or α-tocopherol. C2C12 cells were incubated for 24 h with or without 7β-OHC (50 µM) in the presence or absence of MTSO (100 µg/mL) or α-tocopherol (α-toco, 400 µM). Ultrastructural aspects of peroxisomes, mitochondria and endoplasmic reticulum in untreated cells (control) (**A**), α-tocopherol-treated cells (**C**), and MTSO-treated cells (**E**): numerous mitochondria with regular and homogenous shapes, clear and regular cristae as well as round and regular peroxisomes were detected; the endoplasmic reticulum is also clearly observed. In 7β-OHC-treated cells (**B**), irregular mitochondria with an increased size, reduced matrix density, and disrupted cristae, as well as peroxisomes with abnormal sizes and shapes were visualized. In (7β-OHC + α-tocopherol)-treated cells (**D**) and (7β-OHC+ MTSO)-treated cells (**F**), mainly mitochondria and peroxisomes morphologically similar than those present in the control cells were observed. The white arrows point towards mitochondria, the yellow arrows point towards peroxisomes and the red arrows point towards endoplasmic reticulum.

Figure 3. Attenuation by milk thistle seed oil (MTSO) and α-tocopherol of 7β-hydroxycholesterol-induced changes of the peroxisomal topography, mass and biogenesis on C2C12 cells. C2C12 cells were incubated for 24 h with or without 7β-OHC (50 µM) in the presence or absence of MTSO (100 µg/mL) or α-tocopherol (α-toco, 400 µM). The effect of MTSO and α-tocopherol against 7β-OHC-induced changes of peroxisomal membrane transporter (ABCD3) was analyzed by structured illumination microscopy (apotome) (**A**) as well as flow cytometry (FCM) (**B-C**). The relative gene expression of *Abcd3* (**D**) and *Pex 5* (**E**) mRNAs was determined by real time-quantitative polymerase chain reaction (RT-qPCR). The data are presented as the mean ± SD of two independent experiments performed in triplicate. A multiple comparative analysis between the groups, considering the interactions, was carried out using an ANOVA test followed by a Tukey's test. A p-value less than 0.05 was considered statistically significant. The statistically significant differences between the groups, which are indicated by different letters, consider the vehicle used. **a**: comparison versus control; **b**: comparison versus ETOH (0.5%); **c**: comparison versus DMSO (0.125%); **d**: comparison versus ETOH (0.1%); **e**:

comparison versus (ETOH (0.1%) + DMSO (0.125%)); **f**: comparison versus α-toco (400 µM); **g**: comparison versus MTSO (100 µg/mL); **h**: comparison versus 7β-OHC (50 µM); **i**: comparison versus (7β-OHC (50 µM) + α-toco (400 µM)). No significant differences were observed between untreated cells (control) and vehicle-treated cells.

Figure 4. Effect of milk thistle seed oil (MTSO) and α-tocopherol on the level of ABCD3 peroxisomal transporter and enzymes of the peroxisomal β-oxidation (ACOX1, MFP2) in untreated cells and 7β-hydroxycholesterol-treated C2C12 cells. C2C12 cells were incubated for 24 h with or without 7β-OHC (50 µM) in the presence or absence of MTSO (100 µg/mL) or α-tocopherol (α-toco, 400 µM). Schematic representation of the biochemical pathway of the peroxisomal β-oxidation of very-long-chain fatty acids (VLCFA) (**A**). Peroxisomal β-oxidation was characterized by Western blotting with different antibodies (**B**): transporter, peroxisomal acyl-CoA oxidase 1 (ACOX1), and peroxisomal multifunctional enzyme type 2 (MFP2). The data are presented as the mean ± SD of two independent experiments performed in triplicate and compared with a student's t Test. A p-value less than 0.05 was considered statistically significant. The statistically significant differences are indicated by different symbols: * comparison between MTSO, α-tocopherol, 7β-OHC, and (7β-OHC + MTSO) versus the corresponding vehicle; # comparison between 7β-OHC, (7β-OHC + MTSO) and (7β-OHC + α-toco). No significant differences were observed between untreated cells (control) and vehicle-treated cells.

Figure 5. Attenuation by milk thistle seed oil (MTSO) and α-tocopherol of 7β-hydroxycholesterol-induced accumulation of very-long-chain fatty acids (VLCFA) in C2C12 cells. C2C12 cells were incubated for 24 h with or without 7β-OHC (50 µM) in the presence or absence of MTSO (100 µg/mL) or α-tocopherol (α-toco, 400 µM). The level of VLCFA (C ≥ 22) was determined by GC-MS: C22:0 (**A**), C22:1 n−9 (**B**), C24:0 (**C**), C24:1 n−9 (**D**), C26:0 (**E**) and C26:1 n−9 (**F**). Data are the mean ± SD of two independent experiments. A multiple comparative analysis between the groups, considering the interactions, was carried out using an ANOVA test followed by a Tukey's test. A p-value less than 0.05 was considered statistically significant. The statistically significant differences between the groups, which are

indicated by different letters, consider the vehicle used. **a**: comparison versus control; **b**: comparison versus ETOH (0.5%); **c**: comparison versus DMSO (0.125%); **d**: comparison versus ETOH (0.1%); **e**: comparison versus (ETOH (0.1%) + DMSO (0.125%)); **f**: comparison versus α-toco (400 µM); **g**: comparison versus PLSO (100 µg/mL); **h**: comparison versus 7β-OHC (50 µM); **i**: comparison versus (7β-OHC (50 µM) + α-toco (400 µM)). No significant differences were observed between untreated cells (control) and vehicle-treated cells.

Figure 6. Heatmap representation of the cytoxicity of 7β-hydroxycholesterol and of the cytoprotective effects of milk thistle seed oil (MTSO) and α-tocopherol on C2C12 cells by considering cell death, transmembrane mitochondrial potential, ROS overproduction and peroxisomal status. Heatmap graded from green (little or no effect: 0) to pink (maximum effect: 100).

Supplementary Figure S1: Evaluation of the effects of 7β–hydroxycholesterol, milk thistle seed oil (MTSO) and α–tocopherol on C2C12 cell viability. A: C2C12 cells were incubated with different concentrations of 7β-hydroxycholesterol (7β-OHC) for 24 h, cell viability was determined with the FDA assay; **B**: C2C12 cells were incubated for 24 h with MTSO used at different concentrations, cell viability was determined with the MTT assay; **C**: C2C12 cells were incubated for 24 h with α-tocopherol (α-toco) used at different concentrations, cell viability was determined with the MTT assay,

Supplementary Figure S2: Effect of milk thistle seed oil (MTSO) and α-tocopherol on 7β-hydroxycholesterol-treated C2C12 cells: impact on cell morphology. C2C12 cells were incubated for 24 h with or without 7β-OHC (50 µM) in the presence or absence of MTSO (100 µg/mL) or α-tocopherol (α-toco, 400 µM). The protective effect of MTSO and α-tocopherol against 7β-OH-induced modification of cell growth and morphology were realized by phase-contrast microscopy.

Supplementary Figure S3: Effect of milk thistle seed oil (MTSO) and α-tocopherol on lipid droplets formation. C2C12 cells were cultured for 24 h with or without 7β-OHC (50 μM) in the presence or absence of MTSO (100 μg/mL) or α-tocopherol (α-toco, 400 μM). Oleic acid (OA) was used as positive control to induce lipid droplets formation. The observations were realized under an inverted phase contrast microscope. In these conditions of observation, lipid droplets, localized in the cytoplasm, were only observed in all OA-treated cells and in around 10% of 7β-OHC-treated cells. The points observed in the nuclei correspond to nucleoli.

Supplementary Figure S4: Effect of milk thistle seed oil (MTSO) and α-tocopherol on 7β-hydroxycholesterol-induced changes of peroxisomal biogenesis: measurement of the mRNA levels of Pex13 and Pex14 by real time-quantitative polymerase chain reaction (RT-qPCR).

REFERENCES

[1] E.H. Gordon, R.E. Hubbard, Differences in frailty in older men and women, Med J Aust 212(4) (2020) 183-188.
[2] M. Bhadra, P. Howell, S. Dutta, C. Heintz, W.B. Mair, Alternative splicing in aging and longevity, Hum Genet 139(3) (2020) 357-369.
[3] M. Tosato, V. Zamboni, A. Ferrini, M. Cesari, The aging process and potential interventions to extend life expectancy, Clin Interv Aging 2(3) (2007) 401-12.
[4] E. Jaul, J. Barron, Age-Related Diseases and Clinical and Public Health Implications for the 85 Years Old and Over Population, Front Public Health 5 (2017) 335.
[5] I. Liguori, G. Russo, F. Curcio, G. Bulli, L. Aran, D. Della-Morte, G. Gargiulo, G. Testa, F. Cacciatore, D. Bonaduce, P. Abete, Oxidative stress, aging, and diseases, Clin Interv Aging 13 (2018) 757-772.
[6] C. Izzo, P. Vitillo, P. Di Pietro, V. Visco, A. Strianese, N. Virtuoso, M. Ciccarelli, G. Galasso, A. Carrizzo, C. Vecchione, The Role of Oxidative Stress in Cardiovascular Aging and Cardiovascular Diseases, Life (Basel) 11(1) (2021).
[7] M. Zarbafian, S. Dayan, S.G. Fabi, Teachings from COVID-19 and aging-An oxidative process, J Cosmet Dermatol 19(12) (2020) 3171-3176.
[8] P.A. Grimsrud, H. Xie, T.J. Griffin, D.A. Bernlohr, Oxidative stress and covalent modification of protein with bioactive aldehydes, J Biol Chem 283(32) (2008) 21837-41.
[9] A.K. Hauck, D.A. Bernlohr, Oxidative stress and lipotoxicity, J Lipid Res 57(11) (2016) 1976-1986.
[10] V. Rani, G. Deep, R.K. Singh, K. Palle, U.C. Yadav, Oxidative stress and metabolic disorders: Pathogenesis and therapeutic strategies, Life Sci 148 (2016) 183-93.
[11] V. Mutemberezi, O. Guillemot-Legris, G.G. Muccioli, Oxysterols: From cholesterol metabolites to key mediators, Prog Lipid Res 64 (2016) 152-169.

[12] B.B. Misra, The Chemical Exposome of Human Aging, Front Genet 11 (2020) 574936.
[13] A. Anderson, A. Campo, E. Fulton, A. Corwin, W.G. Jerome, 3rd, M.S. O'Connor, 7-Ketocholesterol in disease and aging, Redox Biol 29 (2020) 101380.
[14] A. Vejux, D. Abed-Vieillard, K. Hajji, A. Zarrouk, J.J. Mackrill, S. Ghosh, T. Nury, A. Yammine, M. Zaibi, W. Mihoubi, H. Bouchab, B. Nasser, Y. Grosjean, G. Lizard, 7-Ketocholesterol and 7β-hydroxycholesterol: In vitro and animal models used to characterize their activities and to identify molecules preventing their toxicity, Biochem Pharmacol 173 (2020) 113648.
[15] A. Zarrouk, A. Vejux, J. Mackrill, Y. O'Callaghan, M. Hammami, N. O'Brien, G. Lizard, Involvement of oxysterols in age-related diseases and ageing processes, Ageing Res Rev 18 (2014) 148-62.
[16] G. Testa, D. Rossin, G. Poli, F. Biasi, G. Leonarduzzi, Implication of oxysterols in chronic inflammatory human diseases, Biochimie 153 (2018) 220-231.
[17] A. Samadi, S. Sabuncuoglu, M. Samadi, S.Y. Isikhan, S. Chirumbolo, M. Peana, I. Lay, A. Yalcinkaya, G. Bjørklund, A Comprehensive Review on Oxysterols and Related Diseases, Current medicinal chemistry 28(1) (2021) 110-136.
[18] I. Ghzaiel, K. Sassi, A. Zarrouk, T. Nury, M. Ksila, V. Leoni, B. Bouhaouala-Zahar, S. Hammami, M. Hammami, J.J. Mackrill, M. Samadi, T. Ghrairi, A. Vejux, G. Lizard, 7-Ketocholesterol: Effects on viral infections and hypothetical contribution in COVID-19, J Steroid Biochem Mol Biol 212 (2021) 105939.
[19] J.B. Lin, A. Sene, A. Santeford, H. Fujiwara, R. Sidhu, M.M. Ligon, V.A. Shankar, N. Ban, I.U. Mysorekar, D.S. Ory, R.S. Apte, Oxysterol Signatures Distinguish Age-Related Macular Degeneration from Physiologic Aging, EBioMedicine 32 (2018) 9-20.
[20] H. Shokr, I.H. Dias, D. Gherghel, Oxysterols and Retinal Microvascular Dysfunction as Early Risk Markers for Cardiovascular Disease in Normal, Ageing Individuals, Antioxidants (Basel) 10(11) (2021).
[21] G. Leonarduzzi, S. Gargiulo, P. Gamba, G. Testa, B. Sottero, D. Rossin, E. Staurenghi, G. Poli, Modulation of cell signaling pathways by oxysterols in age-related human diseases, Free Radic Biol Med 75 Suppl 1 (2014) S5.
[22] I. Ghzaiel, A. Zarrouk, T. Nury, M. Libergoli, F. Florio, S. Hammouda, F. Ménétrier, L. Avoscan, A. Yammine, M. Samadi, N. Latruffe, S. Biressi, D. Levy, S.P. Bydlowski, S. Hammami, A. Vejux, M. Hammami, G. Lizard, Antioxidant Properties and Cytoprotective Effect of Pistacia lentiscus L. Seed Oil against 7β-Hydroxycholesterol-Induced Toxicity in C2C12 Myoblasts: Reduction in Oxidative Stress, Mitochondrial and Peroxisomal Dysfunctions and Attenuation of Cell Death, Antioxidants (Basel) 10(11) (2021).
[23] J.Y. Lim, W.R. Frontera, Single skeletal muscle fiber mechanical properties: a muscle quality biomarker of human aging, Eur J Appl Physiol (2022).
[24] K. Ragot, J.J. Mackrill, A. Zarrouk, T. Nury, V. Aires, A. Jacquin, A. Athias, J.P. Pais de Barros, A. Véjux, J.M. Riedinger, D. Delmas, G. Lizard, Absence of correlation between oxysterol accumulation in lipid raft microdomains, calcium increase, and apoptosis induction on 158N murine oligodendrocytes, Biochem Pharmacol 86(1) (2013) 67-79.
[25] T. Nury, A. Zarrouk, J.J. Mackrill, M. Samadi, P. Durand, J.M. Riedinger, M. Doria, A. Vejux, E. Limagne, D. Delmas, M. Prost, T. Moreau, M. Hammami, R. Delage-Mourroux, N.M. O'Brien, G. Lizard, Induction of oxiapoptophagy on 158N murine oligodendrocytes treated by 7-ketocholesterol-, 7β-hydroxycholesterol-, or 24(S)-hydroxycholesterol: Protective effects of α-tocopherol and docosahexaenoic acid (DHA; C22:6 n-3), Steroids 99(Pt B) (2015) 194-203.
[26] A. Suzuki, Y. Urano, T. Ishida, N. Noguchi, Different functions of vitamin E homologues in the various types of cell death induced by oxysterols, Free Radic Biol Med 176 (2021) 356-365.
[27] L. Abenavoli, R. Capasso, N. Milic, F. Capasso, Milk thistle in liver diseases: past, present, future, Phytother Res 24(10) (2010) 1423-32.
[28] M. Bijak, Silybin, a Major Bioactive Component of Milk Thistle (Silybum marianum L. Gaernt.)-Chemistry, Bioavailability, and Metabolism, Molecules 22(11) (2017).

[29] W. Meddeb, L. Rezig, M. Abderrabba, G. Lizard, M. Mejri, Tunisian Milk Thistle: An Investigation of the Chemical Composition and the Characterization of Its Cold-Pressed Seed Oils, Int J Mol Sci 18(12) (2017).
[30] A. Zarrouk, L. Martine, S. Grégoire, T. Nury, W. Meddeb, E. Camus, A. Badreddine, P. Durand, A. Namsi, A. Yammine, B. Nasser, M. Mejri, L. Bretillon, J.J. Mackrill, M. Cherkaoui-Malki, M. Hammami, G. Lizard, Profile of Fatty Acids, Tocopherols, Phytosterols and Polyphenols in Mediterranean Oils (Argan Oils, Olive Oils, Milk Thistle Seed Oils and Nigella Seed Oil) and Evaluation of their Antioxidant and Cytoprotective Activities, Current pharmaceutical design 25(15) (2019) 1791-1805.
[31] S. Hammouda, I. Ghzaiel, P. Picón-Pagès, W. Meddeb, W. Khamlaoui, S. Hammami, F.J. Muñoz, M. Hammami, A. Zarrouk, Nigella and Milk Thistle Seed Oils: Potential Cytoprotective Effects against 7β-Hydroxycholesterol-Induced Toxicity on SH-SY5Y Cells, Biomolecules 11(6) (2021).
[32] S. Monier, M. Samadi, C. Prunet, M. Denance, A. Laubriet, A. Athias, A. Berthier, E. Steinmetz, G. Jürgens, A. Nègre-Salvayre, G. Bessède, S. Lemaire-Ewing, D. Néel, P. Gambert, G. Lizard, Impairment of the cytotoxic and oxidative activities of 7 beta-hydroxycholesterol and 7-ketocholesterol by esterification with oleate, Biochem Biophys Res Commun 303(3) (2003) 814-24.
[33] T. Nury, A. Zarrouk, A. Vejux, M. Doria, J.M. Riedinger, R. Delage-Mourroux, G. Lizard, Induction of oxiapoptophagy, a mixed mode of cell death associated with oxidative stress, apoptosis and autophagy, on 7-ketocholesterol-treated 158N murine oligodendrocytes: impairment by α-tocopherol, Biochem Biophys Res Commun 446(3) (2014) 714-9.
[34] W. Meddeb, L. Rezig, A. Zarrouk, T. Nury, A. Vejux, M. Prost, L. Bretillon, M. Mejri, G. Lizard, Cytoprotective Activities of Milk Thistle Seed Oil Used in Traditional Tunisian Medicine on 7-Ketocholesterol and 24S-Hydroxycholesterol-Induced Toxicity on 158N Murine Oligodendrocytes, Antioxidants (Basel) 7(7) (2018).
[35] T. Nury, A. Zarrouk, A. Yammine, J.J. Mackrill, A. Vejux, G. Lizard, Oxiapoptophagy: A type of cell death induced by some oxysterols, Br J Pharmacol 178(16) (2021) 3115-3123.
[36] M. Schrader, J.K. Burkhardt, E. Baumgart, G. Lüers, A. Völkl, H.D. Fahimi, The importance of microtubules in determination of shape and intracellular distribution of peroxisomes, Ann N Y Acad Sci 804 (1996) 669-71.
[37] M. Schrader, H.D. Fahimi, Growth and division of peroxisomes, Int Rev Cytol 255 (2006) 237-90.
[38] M. Schrader, H.D. Fahimi, The peroxisome: still a mysterious organelle, Histochem Cell Biol 129(4) (2008) 421-40.
[39] R.J. Wanders, H.R. Waterham, Biochemistry of mammalian peroxisomes revisited, Annu Rev Biochem 75 (2006) 295-332.
[40] R.J. Wanders, Metabolic functions of peroxisomes in health and disease, Biochimie 98 (2014) 36-44.
[41] R.J.A. Wanders, F.M. Vaz, H.R. Waterham, S. Ferdinandusse, Fatty Acid Oxidation in Peroxisomes: Enzymology, Metabolic Crosstalk with Other Organelles and Peroxisomal Disorders, Adv Exp Med Biol 1299 (2020) 55-70.
[42] M. Fransen, C. Lismont, Peroxisomes and Cellular Oxidant/Antioxidant Balance: Protein Redox Modifications and Impact on Inter-organelle Communication, Subcell Biochem 89 (2018) 435-461.
[43] S.R. Terlecky, J.I. Koepke, P.A. Walton, Peroxisomes and aging, Biochim Biophys Acta 1763(12) (2006) 1749-54.
[44] C.R. Giordano, S.R. Terlecky, Peroxisomes, cell senescence, and rates of aging, Biochim Biophys Acta 1822(9) (2012) 1358-62.
[45] M. Fransen, M. Nordgren, B. Wang, O. Apanasets, P.P. Van Veldhoven, Aging, age-related diseases and peroxisomes, Subcell Biochem 69 (2013) 45-65.
[46] G. Lizard, O. Rouaud, J. Demarquoy, M. Cherkaoui-Malki, L. Iuliano, Potential roles of peroxisomes in Alzheimer's disease and in dementia of the Alzheimer's type, J Alzheimers Dis 29(2) (2012) 241-54.

[47] D. Trompier, A. Vejux, A. Zarrouk, C. Gondcaille, F. Geillon, T. Nury, S. Savary, G. Lizard, Brain peroxisomes, Biochimie 98 (2014) 102-10.
[48] A. Zarrouk, T. Nury, H.I. El Hajj, C. Gondcaille, P. Andreoletti, T. Moreau, M. Cherkaoui-Malki, J. Berger, M. Hammami, G. Lizard, A. Vejux, Potential Involvement of Peroxisome in Multiple Sclerosis and Alzheimer's Disease : Peroxisome and Neurodegeneration, Adv Exp Med Biol 1299 (2020) 91-104.
[49] C. Lismont, M. Nordgren, P.P. Van Veldhoven, M. Fransen, Redox interplay between mitochondria and peroxisomes, Front Cell Dev Biol 3 (2015) 35.
[50] G. Nascimento-Dos-Santos, E. de-Souza-Ferreira, R. Linden, A. Galina, H. Petrs-Silva, Mitotherapy: Unraveling a Promising Treatment for Disorders of the Central Nervous System and Other Systemic Conditions, Cells 10(7) (2021).
[51] A.G. Atanasov, S.B. Zotchev, V.M. Dirsch, C.T. Supuran, Natural products in drug discovery: advances and opportunities, Nat Rev Drug Discov 20(3) (2021) 200-216.
[52] L. Santos, The impact of nutrition and lifestyle modification on health, Eur J Intern Med (2021).
[53] M. Debbabi, A. Zarrouk, M. Bezine, W. Meddeb, T. Nury, A. Badreddine, E.M. Karym, R. Sghaier, L. Bretillon, S. Guyot, M. Samadi, M. Cherkaoui-Malki, B. Nasser, M. Mejri, S. Ben-Hammou, M. Hammami, G. Lizard, Comparison of the effects of major fatty acids present in the Mediterranean diet (oleic acid, docosahexaenoic acid) and in hydrogenated oils (elaidic acid) on 7-ketocholesterol-induced oxiapoptophagy in microglial BV-2 cells, Chem Phys Lipids 207(Pt B) (2017) 151-170.
[54] T. Mosmann, Rapid colorimetric assay for cellular growth and survival: application to proliferation and cytotoxicity assays, J Immunol Methods 65(1-2) (1983) 55-63.
[55] G. Lizard, S. Gueldry, V. Deckert, P. Gambert, L. Lagrost, Evaluation of the cytotoxic effects of some oxysterols and of cholesterol on endothelial cell growth: methodological aspects, Pathol Biol (Paris) 45(4) (1997) 281-90.
[56] A. Namsi, T. Nury, A.S. Khan, J. Leprince, D. Vaudry, C. Caccia, V. Leoni, A.G. Atanasov, M.C. Tonon, O. Masmoudi-Kouki, G. Lizard, Octadecaneuropeptide (ODN) Induces N2a Cells Differentiation through a PKA/PLC/PKC/MEK/ERK-Dependent Pathway: Incidence on Peroxisome, Mitochondria, and Lipid Profiles, Molecules 24(18) (2019).
[57] G. Rothe, G. Valet, Flow cytometric analysis of respiratory burst activity in phagocytes with hydroethidine and 2',7'-dichlorofluorescin, J Leukoc Biol 47(5) (1990) 440-8.
[58] T.C. Walther, R.V. Farese, Jr., Lipid droplets and cellular lipid metabolism, Annu Rev Biochem 81 (2012) 687-714.
[59] M. Debbabi, T. Nury, I. Helali, E.M. Karym, F. Geillon, C. Gondcaille, D. Trompier, A. Najid, S. Terreau, M. Bezine, A. Zarrouk, A. Vejux, P. Andreoletti, M. Cherkaoui-Malki, S. Savary, G. Lizard, Flow Cytometric Analysis of the Expression Pattern of Peroxisomal Proteins, Abcd1, Abcd2, and Abcd3 in BV-2 Murine Microglial Cells, Methods Mol Biol 1595 (2017) 257-265.
[60] L. Schepers, P.P. Van Veldhoven, M. Casteels, H.J. Eyssen, G.P. Mannaerts, Presence of three acyl-CoA oxidases in rat liver peroxisomes. An inducible fatty acyl-CoA oxidase, a noninducible fatty acyl-CoA oxidase, and a noninducible trihydroxycoprostanoyl-CoA oxidase, J Biol Chem 265(9) (1990) 5242-6.
[61] S. Savary, D. Trompier, P. Andréoletti, F. Le Borgne, J. Demarquoy, G. Lizard, Fatty acids - induced lipotoxicity and inflammation, Curr Drug Metab 13(10) (2012) 1358-70.
[62] J. Blondelle, J.P. Pais de Barros, F. Pilot-Storck, L. Tiret, Targeted Lipidomic Analysis of Myoblasts by GC-MS and LC-MS/MS, Methods Mol Biol 1668 (2017) 39-60.
[63] J. Folch, M. Lees, G.H. Sloane Stanley, A simple method for the isolation and purification of total lipides from animal tissues, J Biol Chem 226(1) (1957) 497-509.
[64] S. Dzeletovic, O. Breuer, E. Lund, U. Diczfalusy, Determination of cholesterol oxidation products in human plasma by isotope dilution-mass spectrometry, Anal Biochem 225(1) (1995) 73-80.
[65] V. Leoni, T. Nury, A. Vejux, A. Zarrouk, C. Caccia, M. Debbabi, A. Fromont, R. Sghaier, T. Moreau, G. Lizard, Mitochondrial dysfunctions in 7-ketocholesterol-treated 158N oligodendrocytes without or with

α-tocopherol: Impacts on the cellular profil of tricarboxylic cycle-associated organic acids, long chain saturated and unsaturated fatty acids, oxysterols, cholesterol and cholesterol precursors, J Steroid Biochem Mol Biol 169 (2017) 96-110.
[66] R.J. Wanders, J.M. Tager, Lipid metabolism in peroxisomes in relation to human disease, Mol Aspects Med 19(2) (1998) 69-154.
[67] M. Fransen, M. Nordgren, B. Wang, O. Apanasets, Role of peroxisomes in ROS/RNS-metabolism: implications for human disease, Biochim Biophys Acta 1822(9) (2012) 1363-73.
[68] A. Sugiura, S. Mattie, J. Prudent, H.M. McBride, Newly born peroxisomes are a hybrid of mitochondrial and ER-derived pre-peroxisomes, Nature 542(7640) (2017) 251-254.
[69] E. Gray, C. Rice, K. Hares, J. Redondo, K. Kemp, M. Williams, A. Brown, N. Scolding, A. Wilkins, Reductions in neuronal peroxisomes in multiple sclerosis grey matter, Mult Scler 20(6) (2014) 651-9.
[70] W. Wang, S. Subramani, Role of PEX5 ubiquitination in maintaining peroxisome dynamics and homeostasis, Cell Cycle 16(21) (2017) 2037-2045.
[71] J.Y. Wang, L. Li, R.Y. Chai, H.P. Qiu, Z. Zhang, Y.L. Wang, X.H. Liu, F.C. Lin, G.C. Sun, Pex13 and Pex14, the key components of the peroxisomal docking complex, are required for peroxisome formation, host infection and pathogenicity-related morphogenesis in Magnaporthe oryzae, Virulence 10(1) (2019) 292-314.
[72] S. Hein, P. Schönfeld, S. Kahlert, G. Reiser, Toxic effects of X-linked adrenoleukodystrophy-associated, very long chain fatty acids on glial cells and neurons from rat hippocampus in culture, Hum Mol Genet 17(12) (2008) 1750-61.
[73] M. Baarine, P. Andréoletti, A. Athias, T. Nury, A. Zarrouk, K. Ragot, A. Vejux, J.M. Riedinger, Z. Kattan, G. Bessede, D. Trompier, S. Savary, M. Cherkaoui-Malki, G. Lizard, Evidence of oxidative stress in very long chain fatty acid--treated oligodendrocytes and potentialization of ROS production using RNA interference-directed knockdown of ABCD1 and ACOX1 peroxisomal proteins, Neuroscience 213 (2012) 1-18.
[74] F.A. de Freitas, D. Levy, A. Zarrouk, G. Lizard, S.P. Bydlowski, Impact of Oxysterols on Cell Death, Proliferation, and Differentiation Induction: Current Status, Cells 10(9) (2021).
[75] A. Vejux, G. Lizard, Cytotoxic effects of oxysterols associated with human diseases: Induction of cell death (apoptosis and/or oncosis), oxidative and inflammatory activities, and phospholipidosis, Mol Aspects Med 30(3) (2009) 153-70.
[76] H. Xu, S. Zhou, Q. Tang, H. Xia, F. Bi, Cholesterol metabolism: New functions and therapeutic approaches in cancer, Biochim Biophys Acta Rev Cancer 1874(1) (2020) 188394.
[77] G. Poli, F. Biasi, G. Leonarduzzi, Oxysterols in the pathogenesis of major chronic diseases, Redox Biol 1(1) (2013) 125-30.
[78] S. Saberianpour, A. Karimi, M.H. Saeed Modaghegh, M. Ahmadi, Different types of cell death in vascular diseases, Mol Biol Rep 48(5) (2021) 4687-4702.
[79] C.S. Chambers, V. Holečková, L. Petrásková, D. Biedermann, K. Valentová, M. Buchta, V. Křen, The silymarin composition… and why does it matter???, Food Res Int 100(Pt 3) (2017) 339-353.
[80] T. Nury, A. Yammine, I. Ghzaiel, K. Sassi, A. Zarrouk, F. Brahmi, M. Samadi, S. Rup-Jacques, D. Vervandier-Fasseur, J.P. Pais de Barros, V. Bergas, S. Ghosh, M. Majeed, A. Pande, A. Atanasov, S. Hammami, M. Hammami, J. Mackrill, B. Nasser, P. Andreoletti, M. Cherkaoui-Malki, A. Vejux, G. Lizard, Attenuation of 7-ketocholesterol- and 7β-hydroxycholesterol-induced oxiapoptophagy by nutrients, synthetic molecules and oils: Potential for the prevention of age-related diseases, Ageing Res Rev 68 (2021) 101324.
[81] M. Fransen, C. Lismont, P. Walton, The Peroxisome-Mitochondria Connection: How and Why?, Int J Mol Sci 18(6) (2017).
[82] Y. Saito, Diverse cytoprotective actions of vitamin E isoforms- role as peroxyl radical scavengers and complementary functions with selenoproteins, Free Radic Biol Med 175 (2021) 121-129.

[83] E. Pedruzzi, C. Guichard, V. Ollivier, F. Driss, M. Fay, C. Prunet, J.C. Marie, C. Pouzet, M. Samadi, C. Elbim, Y. O'Dowd, M. Bens, A. Vandewalle, M.A. Gougerot-Pocidalo, G. Lizard, E. Ogier-Denis, NAD(P)H oxidase Nox-4 mediates 7-ketocholesterol-induced endoplasmic reticulum stress and apoptosis in human aortic smooth muscle cells, Mol Cell Biol 24(24) (2004) 10703-17.
[84] C.L. Fattman, L.M. Schaefer, T.D. Oury, Extracellular superoxide dismutase in biology and medicine, Free Radic Biol Med 35(3) (2003) 236-56.
[85] A. Thoma, T. Akter-Miah, R.L. Reade, A.P. Lightfoot, Targeting reactive oxygen species (ROS) to combat the age-related loss of muscle mass and function, Biogerontology 21(4) (2020) 475-484.
[86] V.M. Olkkonen, R. Hynynen, Interactions of oxysterols with membranes and proteins, Mol Aspects Med 30(3) (2009) 123-33.
[87] J.M. Zahm, S. Baconnais, S. Monier, N. Bonnet, G. Bessède, P. Gambert, E. Puchelle, G. Lizard, Chronology of cellular alterations during 7-ketocholesterol-induced cell death on A7R5 rat smooth muscle cells: analysis by time lapse-video microscopy and conventional fluorescence microscopy, Cytometry A 52(2) (2003) 57-69.
[88] R. Sghaier, T. Nury, V. Leoni, C. Caccia, J.P. Pais De Barros, A. Cherif, A. Vejux, T. Moreau, K. Limem, M. Samadi, J.J. Mackrill, A.S. Masmoudi, G. Lizard, A. Zarrouk, Dimethyl fumarate and monomethyl fumarate attenuate oxidative stress and mitochondrial alterations leading to oxiapoptophagy in 158N murine oligodendrocytes treated with 7β-hydroxycholesterol, J Steroid Biochem Mol Biol 194 (2019) 105432.
[89] R. Quintana-Cabrera, A. Mehrotra, G. Rigoni, M.E. Soriano, Who and how in the regulation of mitochondrial cristae shape and function, Biochem Biophys Res Commun 500(1) (2018) 94-101.
[90] S. Kemp, F.L. Theodoulou, R.J. Wanders, Mammalian peroxisomal ABC transporters: from endogenous substrates to pathology and clinical significance, Br J Pharmacol 164(7) (2011) 1753-66.
[91] A. D'Amico, E. Bertini, Metabolic neuropathies and myopathies, Handb Clin Neurol 113 (2013) 1437-55.
[92] A. Badreddine, A. Zarrouk, E.M. Karym, M. Debbabi, T. Nury, W. Meddeb, R. Sghaier, M. Bezine, A. Vejux, L. Martine, S. Grégoire, L. Bretillon, E. Prost-Camus, P. Durand, M. Prost, T. Moreau, M. Cherkaoui-Malki, B. Nasser, G. Lizard, Argan Oil-Mediated Attenuation of Organelle Dysfunction, Oxidative Stress and Cell Death Induced by 7-Ketocholesterol in Murine Oligodendrocytes 158N, Int J Mol Sci 18(10) (2017).
[93] T. Nury, R. Sghaier, A. Zarrouk, F. Ménétrier, T. Uzun, V. Leoni, C. Caccia, W. Meddeb, A. Namsi, K. Sassi, W. Mihoubi, J.M. Riedinger, M. Cherkaoui-Malki, T. Moreau, A. Vejux, G. Lizard, Induction of peroxisomal changes in oligodendrocytes treated with 7-ketocholesterol: Attenuation by α-tocopherol, Biochimie 153 (2018) 181-202.
[94] T. Nury, A. Zarrouk, K. Ragot, M. Debbabi, J.M. Riedinger, A. Vejux, P. Aubourg, G. Lizard, 7-Ketocholesterol is increased in the plasma of X-ALD patients and induces peroxisomal modifications in microglial cells: Potential roles of 7-ketocholesterol in the pathophysiology of X-ALD, J Steroid Biochem Mol Biol 169 (2017) 123-136.
[95] A. Yammine, A. Zarrouk, T. Nury, A. Vejux, N. Latruffe, D. Vervandier-Fasseur, M. Samadi, J.J. Mackrill, H. Greige-Gerges, L. Auezova, G. Lizard, Prevention by Dietary Polyphenols (Resveratrol, Quercetin, Apigenin) Against 7-Ketocholesterol-Induced Oxiapoptophagy in Neuronal N2a Cells: Potential Interest for the Treatment of Neurodegenerative and Age-Related Diseases, Cells 9(11) (2020).
[96] N.E. Uzor, D.M. Scheihing, G.S. Kim, J.F. Moruno-Manchon, L. Zhu, C.R. Reynolds, J.M. Stephenson, A. Holmes, L.D. McCullough, A.S. Tsvetkov, Aging lowers PEX5 levels in cortical neurons in male and female mouse brains, Mol Cell Neurosci 107 (2020) 103536.
[97] F.C. Klouwer, K. Berendse, S. Ferdinandusse, R.J. Wanders, M. Engelen, B.T. Poll-The, Zellweger spectrum disorders: clinical overview and management approach, Orphanet J Rare Dis 10 (2015) 151.

[98] L. Jiang, S. Hara-Kuge, S. Yamashita, Y. Fujiki, Peroxin Pex14p is the key component for coordinated autophagic degradation of mammalian peroxisomes by direct binding to LC3-II, Genes Cells 20(1) (2015) 36-49.
[99] M.Y. Lee, R. Sumpter, Jr., Z. Zou, S. Sirasanagandla, Y. Wei, P. Mishra, H. Rosewich, D.I. Crane, B. Levine, Peroxisomal protein PEX13 functions in selective autophagy, EMBO Rep 18(1) (2017) 48-60.
[100] R.J. Wanders, S. Ferdinandusse, P. Brites, S. Kemp, Peroxisomes, lipid metabolism and lipotoxicity, Biochim Biophys Acta 1801(3) (2010) 272-80.
[101] A.P. Bailey, G. Koster, C. Guillermier, E.M. Hirst, J.I. MacRae, C.P. Lechene, A.D. Postle, A.P. Gould, Antioxidant Role for Lipid Droplets in a Stem Cell Niche of Drosophila, Cell 163(2) (2015) 340-53.
[102] J.D. Pressly, M.Z. Gurumani, J.T. Varona Santos, A. Fornoni, S. Merscher, H. Al-Ali, Adaptive and maladaptive roles of lipid droplets in health and disease, Am J Physiol Cell Physiol (2022).
[103] P. Calle, A. Muñoz, A. Sola, G. Hotter, CPT1a gene expression reverses the inflammatory and anti-phagocytic effect of 7-ketocholesterol in RAW264.7 macrophages, Lipids Health Dis 18(1) (2019) 215.
[104] E. Kahn, A. Vejux, D. Dumas, T. Montange, F. Frouin, V. Robert, J.M. Riedinger, J.F. Stoltz, P. Gambert, A. Todd-Pokropek, G. Lizard, FRET multiphoton spectral imaging microscopy of 7-ketocholesterol and Nile Red in U937 monocytic cells loaded with 7-ketocholesterol, Anal Quant Cytol Histol 26(6) (2004) 304-13.
[105] A. Vejux, E. Kahn, D. Dumas, G. Bessède, F. Ménétrier, A. Athias, J.M. Riedinger, F. Frouin, J.F. Stoltz, E. Ogier-Denis, A. Todd-Pokropek, G. Lizard, 7-Ketocholesterol favors lipid accumulation and colocalizes with Nile Red positive cytoplasmic structures formed during 7-ketocholesterol-induced apoptosis: analysis by flow cytometry, FRET biphoton spectral imaging microscopy, and subcellular fractionation, Cytometry A 64(2) (2005) 87-100.
[106] T. Nury, A. Yammine, F. Menetrier, A. Zarrouk, A. Vejux, G. Lizard, 7-Ketocholesterol- and 7β-Hydroxycholesterol-Induced Peroxisomal Disorders in Glial, Microglial and Neuronal Cells: Potential Role in Neurodegeneration : 7-ketocholesterol and 7β-hydroxycholesterol-Induced Peroxisomal Disorders and Neurodegeneration, Adv Exp Med Biol 1299 (2020) 31-41.
[107] A. Badreddine, A. Zarrouk, W. Meddeb, T. Nury, L. Rezig, M. Debbabi, F.Z. Bessam, F. Brahmi, A. Vejux, M. Mejri, B. Nasser, G. Lizard, Chapter 10 - Antioxidant and neuroprotective properties of Mediterranean oils: Argan oil, olive oil, and milk thistle seed oil, in: C.R. Martin, V.R. Preedy (Eds.), Oxidative Stress and Dietary Antioxidants in Neurological Diseases, Academic Press2020, pp. 143-154.
[108] F. Brahmi, A. Vejux, R. Sghaier, A. Zarrouk, T. Nury, W. Meddeb, L. Rezig, A. Namsi, K. Sassi, A. Yammine, I. Badreddine, D. Vervandier-Fasseur, K. Madani, L. Boulekbache-Makhlouf, B. Nasser, G. Lizard, Prevention of 7-ketocholesterol-induced side effects by natural compounds, Crit Rev Food Sci Nutr 59(19) (2019) 3179-3198.

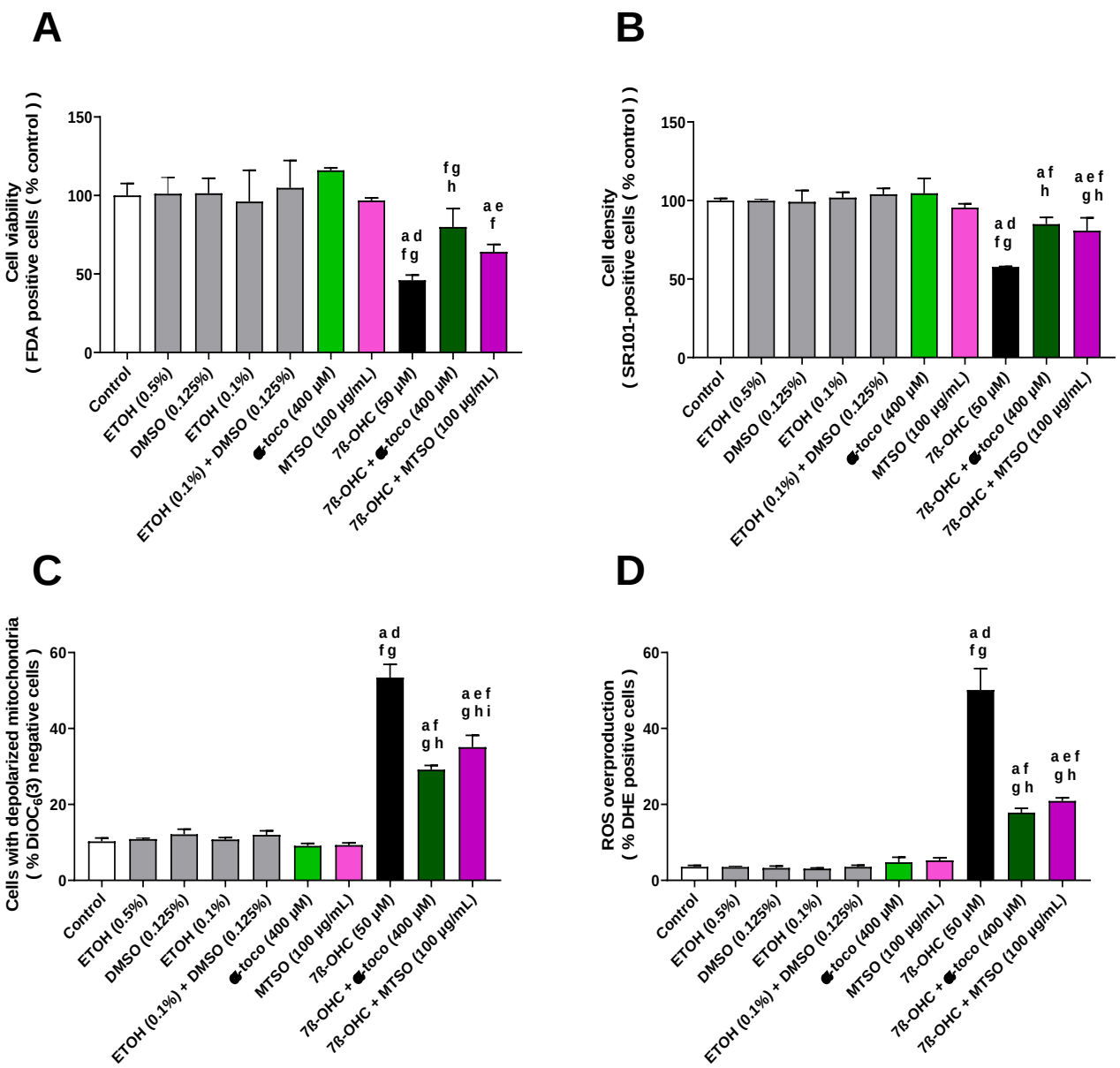

Figure 1

Imen Ghzaiel *et al.*

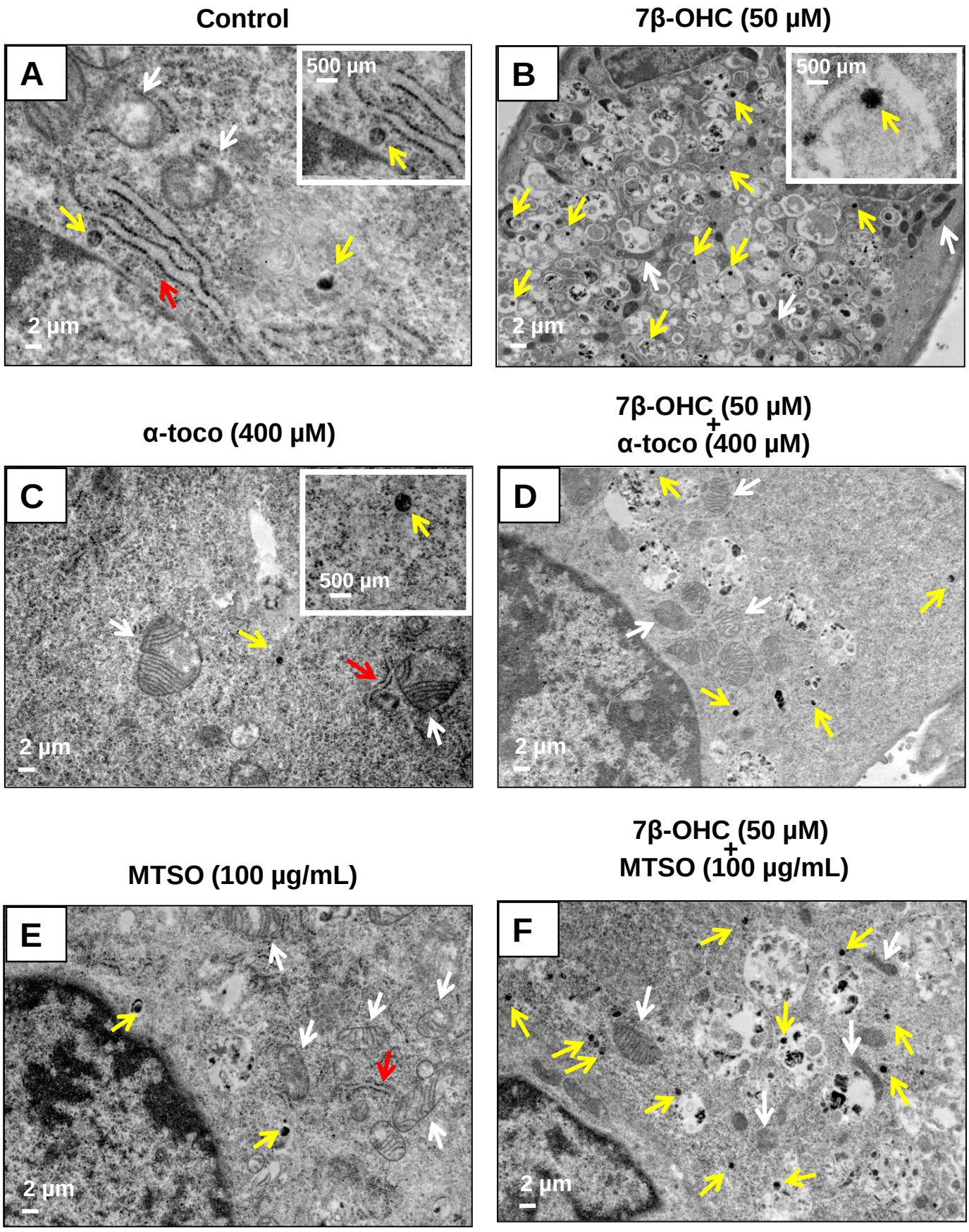

Figure 2

Imen Ghzaiel *et al.*

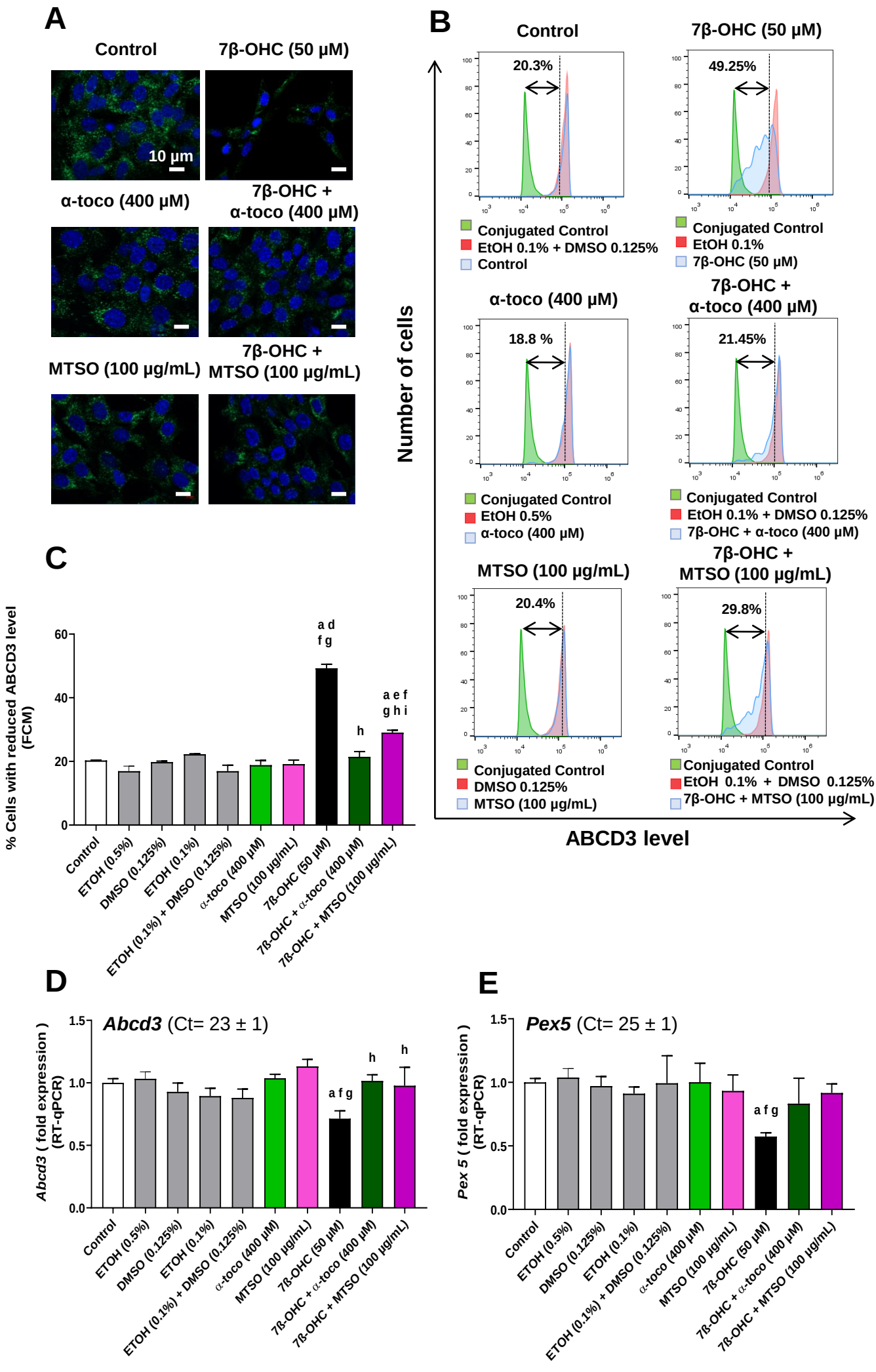

Figure 3

Imen Ghzaiel *et al.*

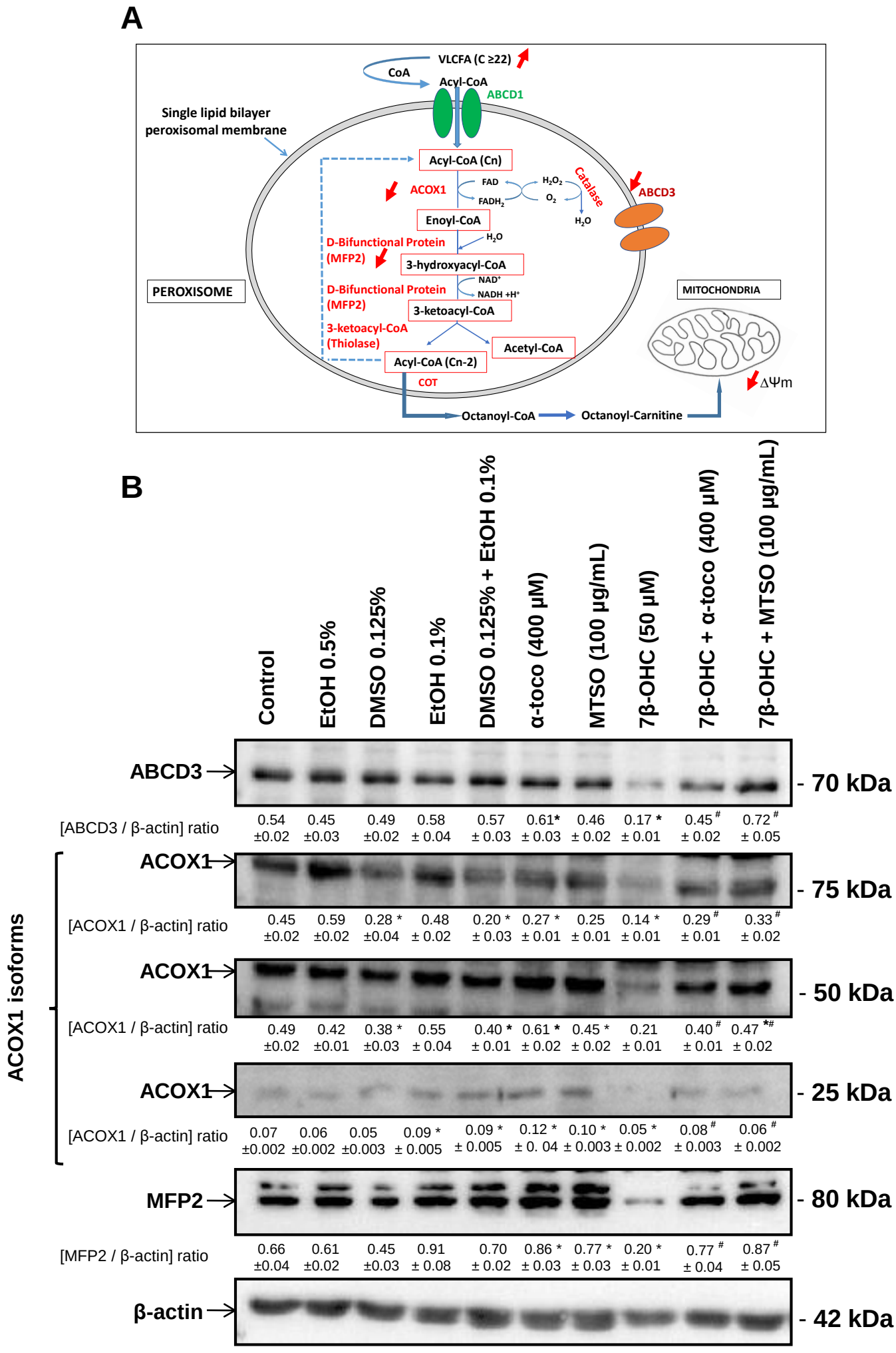

Figure 4
Imen Ghzaiel *et al.*

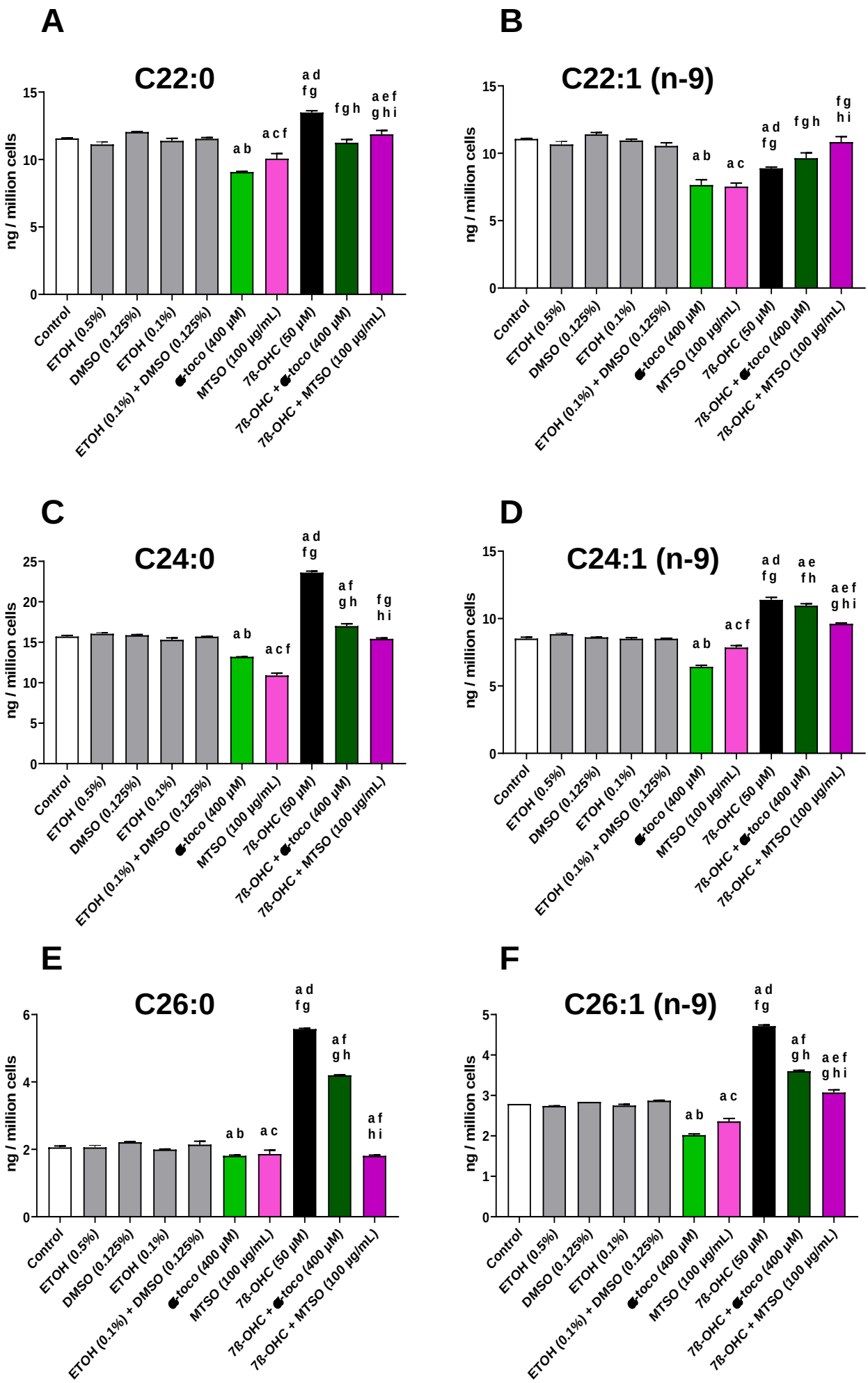

Figure 5; Imen Ghzaiel *et al.*

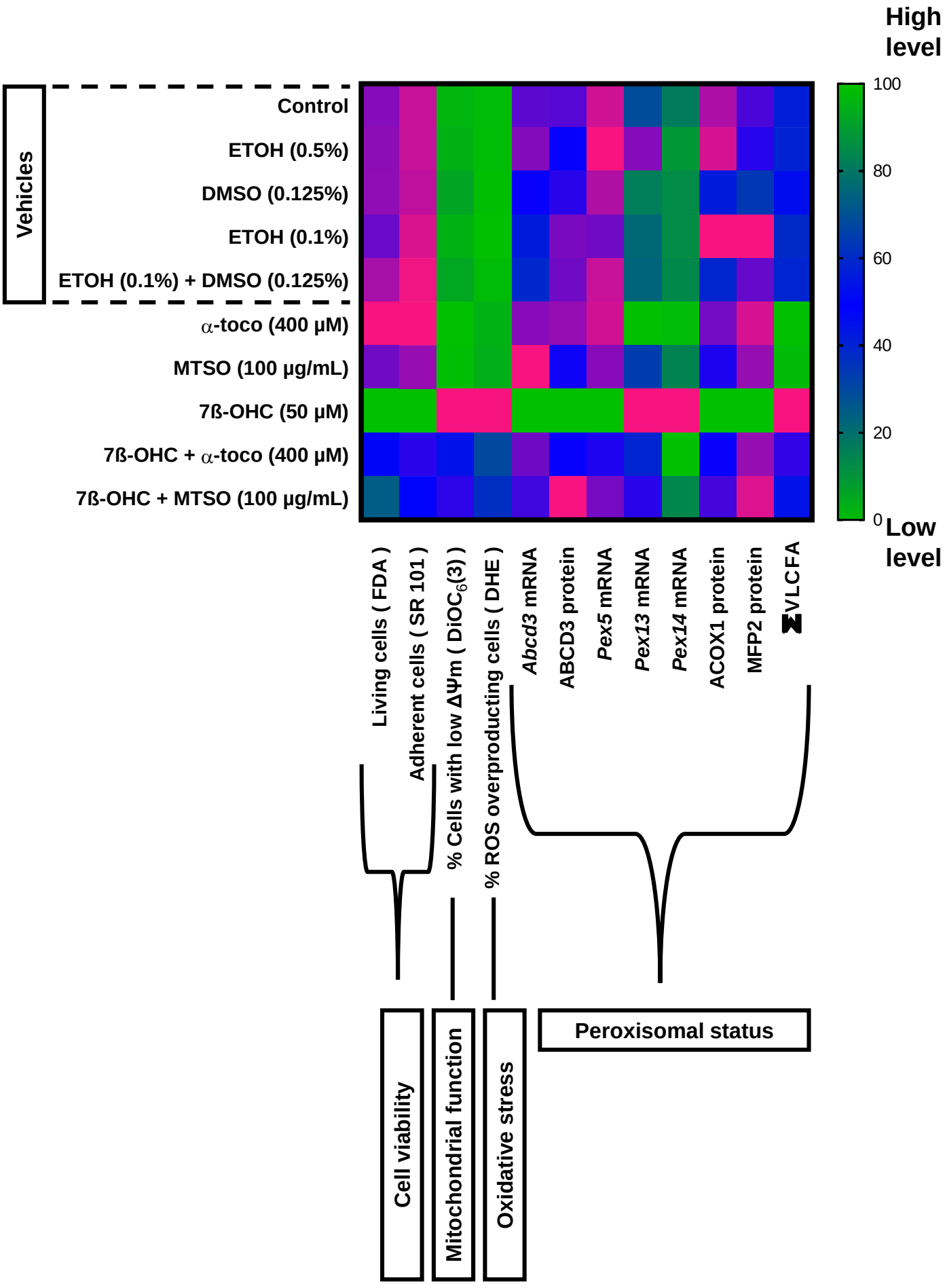

Figure 6
Imen Ghzaiel *et al.*

Table1. Phytochemical profile of milk thistle seed oil (MTSO) from Tunisia

	MTSO (Sousse-Tunisia)
Fatty acid content (% of total fatty acids)	
∑UFA	80.83 ± 1.86
	56.77 ± 0.57% linoleic acid; 21.39 ± 0.02 % oleic acid
∑SFA	19.24 ± 0.17
	13.06 ± 0.07% palmitic acic
Tocopherol content (mg/kg of oil)	
Total tocopherol content	274 ± 24
α-tocopherol	190 ± 20
Phytosterol content (mg/kg of oil)	
Total phytosterol content	5891 ± 118
Polyphenol content (mg equivalent quercetin / kg of oil)	
Vanillin	3.30 ± 0.01

The data presented in the table are extracted from Wiem Meddeb's PhD thesis (Université de Bourgogne Franche-Comté, Dijon, France; title: 'Extraction, caractérisation physicochimique, profil lipidique et activité cytoprotectrice d'huiles de Chardon-Marie de Tunisie', 2018) as well as from previous works realized in the laboratory [29, 30]. UFA: unsaturated fatty acids, SFA: saturated fatty acids. In the MTSO used (Sousse, Tunisia), among tocopherols, α-tocopherol was present in highest quantity [30]. The following phytosterols were mainly present: β-sitosterol > campesterol > schotenol > stigmasterol > Δ5 avenasterol [30]. Vanillin was the only polyphenol identified [29].

Table 2. Accumulation of 7β-hydroxycholesterol in C2C12 cells exposed to 7β-OHC (7β-OHC) with or without α-tocopherol (α-toco) or milk thistle seed oil (MTSO)

	7β-OHC (ng/million cells)
Control	1.24 ± 0.02
ETOH (0.5%)	1.73 ± 0.03
DMSO (0.125%)	2.28 ± 0.03
ETOH (0.1%)	1.45 ± 0.02
ETOH (0.1%) + DMSO (0.125%)	1.42 ± 0.01
α-toco (400 µM)	0.60 ± 0.01
MTSO (100 µg/mL)	2.70 ± 0.04
7β-OHC (50 µM)	3972.84 ± 84.59 [a f g h]
7β-OHC + α-toco (400 µM)	1699.09 ± 6.90 [a f i]
7β-OHC + MTSO (100 µg/mL)	3196.43 ± 96.05 [a e g i j]

Data are the mean ± SD of two independent experiments realized in triplicate. A multiple comparative analysis between the groups, taking into account the interactions, was carried out using an ANOVA test followed by a Tukey's test. As *Pistacia Lentiscus* L. seed oil (PLSO) also showed cytoprotective activities against 7β-OHC-induced cytotoxic effects [22], the accumulation of 7β-OHC was also measured with this oil. Noteworthy, in the presence of PLSO, the cellular concentration of 7β-OHC was similar than in control cells (PLSO 1.36 ± 0.03). However, when PLSO was associated with 7β-OHC, the intracellular accumulation of 7β-OHC was twice lower than with MTSO (7β-OHC + PLSO (100 µg/mL): 1880.13 ± 68.91 [a e h i k]) and in the same range than with α-tocopherol. A p-value less than 0.05 was considered statistically significant. The statistically significant differences between the groups, which are indicated by different letters, take into account the vehicle used. **a**: comparison versus control; **b**: comparison versus ETOH (0.5%); **c**: comparison versus DMSO (0.125%); **d**: comparison versus ETOH (0.1%); **e**: comparison versus (ETOH (0.1%) + DMSO (0.125%)); **f**: comparison versus α-toco (400 µM); **g**: comparison versus MTSO (100 µg/mL); **h**: comparison versus PLSO (100 µg/mL), **i :** comparison versus 7β-OHC (50 µM); **j**: comparison versus (7β-OHC (50 µM) + α-toco (400 µM)) ; **k**: comparison versus (7β-OHC (50 µM) + MTSO (100 µg/mL)). No significant differences were observed between untreated cells (control) and vehicle-treated cells. ETOH: ethanol.

Sarcopenia

Increased plasma level of 7β-hydroxycholesterol (7β-OHC)

Milk thistle seed oil *(Sylibum marianum)*

7β-OHC

α-tocopherol

C2C12 myoblasts

Biogenesis

Pex5

5

VLCFA (C ≥ 22)

Pex 14

Pex 13

Docking complex

ABCD3

ACOX1

MFP2

β-oxidation

Oxidative stress

ROS

❖Topographical modifications
❖Morphological alterations
❖Functional alterations

❖Loss of ΔΨm
❖Morphological alterations

Peroxisome (pexotherapy)

Mitochondria (mitotherapy)

Cell death